

**SYNACCRETIONARY SEDIMENTARY AND VOLCANIC ROCKS IN THE
ORDOVICIAN TETAGOUCHE BACKARC BASIN, NEW BRUNSWICK,
CANADA: EVIDENCE FOR A TRANSITION FROM FOREDEEP TO
FOREARC BASIN SEDIMENTATION**

REGINALD A. WILSON*[†], CEES R. VAN STAAL**,
and WILLIAM C. McCLELLAND***

ABSTRACT. Development of an Upper Ordovician to lower Silurian (Llandovery) accretionary wedge (Brunswick subduction complex) along the composite Laurentian margin accompanied subduction of the Tetagouche backarc basin and coincided with synaccretionary sedimentation in the Bathurst and Fournier supergroups in northern New Brunswick. These dominantly turbiditic synaccretionary units conformably to unconformably overlie Upper Ordovician pelagic shale and chert in the upper stratigraphic levels of several of the nappes that compose the imbricate thrust stack of the subduction complex. Local occurrences of tectonic *mélange* at the contacts between the turbidites and their pelagic substrate are consistent with deposition of at least some of the former during thrust-related deformation in the accretionary wedge. Detrital zircon data indicate maximum depositional ages ranging from 454 ± 3 to 459 ± 8 Ma, coeval with initiation of subduction of the Tetagouche backarc basin. In the Elmtree inlier, arc tholeiitic basalt disconformably or unconformably overlies Darriwilian MORB-type pillowed flows that constitute backarc oceanic crust of the Tetagouche basin. Sedimentary rocks immediately below and intercalated with the arc tholeiites contain detrital zircons ranging from 444 ± 6 Ma to 455 ± 10 Ma, suggesting that the tholeiites are related to backarc subduction.

Detrital zircon age spectra from all sampled units exhibit a distinct Laurentian signature, indicating an abrupt change in provenance coeval with closure of the backarc basin and Ganderia – Laurentia collision. The lithology and implied ages of the Bathurst and Fournier synaccretionary sedimentary rocks support a correlation with siliciclastic and carbonate-rich turbidites of the Matapedia cover sequence, which were deposited farther west in a forearc setting (Matapedia forearc) with respect to subduction of Tetagouche backarc oceanic lithosphere. The implication of Late Ordovician influx onto the accretionary wedge and foredeep of sediments having a Laurentian affiliation (like those in the Matapedia forearc), demonstrates trenchward migration of forearc sedimentation between *ca.* 450 and 430 Ma. This southeastward (present coordinates) expansion occurred in concert with episodic accretion of buoyant crustal blocks that populated the Tetagouche – Exploits basin, and concomitant southeastward step-back of the subduction zone.

Key words: synaccretionary, detrital zircon, Popelogan arc, Tetagouche backarc, Matapedia forearc, Brunswick subduction complex, Bathurst Supergroup, Fournier Supergroup, Ganderia, Salinic orogeny, turbidites

INTRODUCTION

The Early Paleozoic evolution of the northern Appalachians records the opening and closing of the Iapetus ocean between the opposing Laurentian and Gondwanan margins (van Staal and others, 1998, 2009). Coincident with closure, a series of oceanic and continental arcs, back-arcs and microcontinents successively collided with Laurentia

* Geological Surveys Branch, New Brunswick Department of Energy and Mines, PO Box 50, Bathurst, New Brunswick, Canada, E2A 3Z1

** Pacific Division, Geological Survey of Canada, 605 Robson Street, Vancouver, British Columbia, Canada, V6B 5J3

*** Department of Earth and Environmental Sciences, 121 Trowbridge Hall, University of Iowa, Iowa City, Iowa, 52242, USA

[†] Corresponding author: Reg.WILSON@gnb.ca

and resulted in episodic, Early Ordovician to Early Devonian orogenesis, the locus of which shifted progressively southeastward (present coordinates) over time. One of the accreted continental blocks was Ganderia, which rifted from the Amazonian margin of Gondwana at *ca.* 505 Ma (van Staal and others, 1996, 2009, 2012). Southeast-directed subduction of Iapetan oceanic crust along Ganderia's leading edge led to successive construction of the Penobscot (*ca.* 515–480 Ma) and Popelogan (*ca.* 478–453 Ma) arcs and formation of backarc basins (van Staal and others, 2009; Zagorevski and others, 2010; Fyffe and others, 2011). The Tetagouche backarc basin developed in the Middle to Late Ordovician by extension of Ganderian continental crust and rifting of the Popelogan arc. Volcanic and sedimentary rocks associated with extension and rifting of the Popelogan arc, and spreading in the Tetagouche backarc basin, are assigned, respectively, to the Bathurst and Fournier supergroups in the Miramichi and Elmtree inliers of northern New Brunswick (fig. 1). In New Brunswick, pre-backarc rifting volcanic rocks of the Popelogan arc (Meductic Group) are preserved in the Woodstock area, whereas post-rifting arc volcanism is represented by the Balmoral Group, mainly in the Popelogan inlier (fig. 1).

The evolution of the Popelogan arc, from its Early Ordovician origins to its collision with composite Laurentia (that is, the Notre Dame belt; fig. 1) in the Late Ordovician (*ca.* 450–455 Ma) has been described by van Staal and others (1998, 2003, 2009, 2016). The collision of the composite Laurentian margin and the leading peri-Gondwanan element (the Ganderian Popelogan arc) marks the end of the Taconic orogenic cycle. Continued convergence of Ganderia was accommodated by a subduction polarity reversal and northwest-directed subduction of Tetagouche backarc lithosphere beneath composite Laurentia between the Late Ordovician and middle Silurian (*ca.* 450–430 Ma; van Staal, 1987, 1994). (Note that, in this paper, 'early' and 'lower' Silurian refer to the Llandoveryan epoch/series, and 'middle' Silurian to the Wenlockian epoch/series). Subduction of Tetagouche backarc crust was accompanied by development of an accretionary wedge (Brunswick subduction complex) comprising a series of stacked thrust nappes that encompass all rocks of the Fournier and Bathurst supergroups. Deformation of the accretionary wedge marks the beginning of the Salinic orogenic cycle, which culminated in Ganderia – Laurentia collision at *ca.* 430 Ma with entry of the buoyant Gander margin into the subduction zone. Evolution of the Brunswick subduction complex, including temperature-pressure pathways, formation of a distinctive belt of blueschist, timing of nappe emplacement, and evidence for its structural exhumation and erosion, has been described by van Staal and others (1990, 2001, 2003, 2008, 2009).

Middle Ordovician volcanic units of the Fournier and Bathurst supergroups are overlain by Upper Ordovician deep marine sedimentary rocks, consisting mainly of varicolored chert and overlying dark gray to black shale. This pelagic – hemipelagic blanket is regionally widespread within Ganderia and can be traced from Newfoundland into New England (fig. 1); it records true oceanic conditions, distinguished by a lack of clastic input, in the Tetagouche backarc basin immediately prior to and following initiation of northwest-directed subduction at *ca.* 450 Ma. In spite of the submarine conditions that must have continued to prevail as the subduction complex evolved between the Late Ordovician (*ca.* late Katian) and early Wenlockian, sedimentary rocks overlying early to mid Katian shale and chert have been very poorly documented or simply unrecognized as distinct units, with the exception of the Tomogonops Formation (Langton, 1993).

This paper describes three newly-recognized belts of clastic, dominantly turbiditic sedimentary rocks in the Bathurst and Fournier supergroups; these units, along with the Tomogonops Formation, each constitute the youngest rocks in the local stratigraphic succession in which they occur. All four units conformably to unconformably

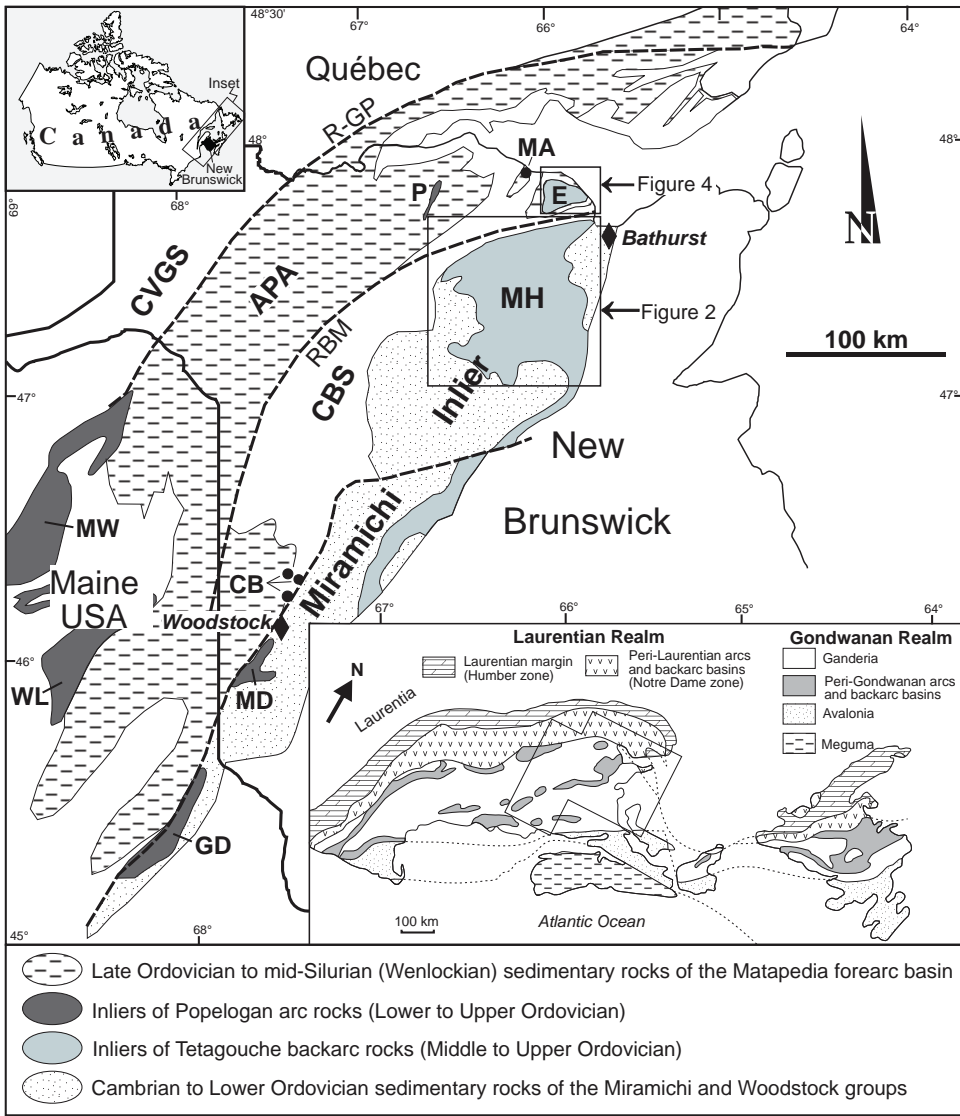


Fig. 1. Location map showing the major geological elements of northwestern New Brunswick. The Matapedia cover sequence comprises three zones (after Rodgers, 1970): CVGS: Connecticut Valley – Gaspé Synclinorium; APA: Aroostook – Percé Anticlinorium; and CBS: Chaleur Bay Synclinorium. Sedimentary rocks of the Matapedia forearc basin (dashed pattern) are restricted to the Aroostook – Percé zone. Volcanic and sedimentary rocks of the Tetagouche backarc basin are exposed in the Miramichi Highlands (MH) and Elmtree inlier (E), whereas dominantly volcanic rocks of the Popelogan arc are exposed in the Popelogan (P), Meductic (MD), Weeksboro – Lunksoos (WL) and Munsungan – Winterville (MW) inliers, below the Matapedia cover rocks. CB: small inliers of the Middle Ordovician Craig Brook Formation; MA: small inlier of Matapedia forearc rocks; RBM: Rocky Brook – Millstream Fault; R-GP: Restigouche – Grand Pabos Fault. Inset: Lithotectonic divisions of the northern Appalachians, after Hibbard and others (2006).

overlie and are locally in tectonic contact with older rocks of the Bathurst and Fournier supergroups, although all have also been incorporated, to some extent, in the Brunswick subduction complex because they are at least locally deformed by D₁ (van Staal and others, 2001). We report detrital zircon data that support syntectonic

deposition of these rocks during progressive deformation in the Brunswick subduction complex, and a linkage with coeval, Laurentia-derived sedimentary rocks of the Matapedia basin, situated farther west (fig. 1) in the forearc region with respect to subduction of Tetagouche backarc crust. We show that these lithological and detrital zircon data signal an abrupt Late Ordovician influx of siliciclastic sediment onto the accretionary wedge and adjacent foredeep; these siliciclastic sedimentary rocks display a Laurentian provenance, demonstrating trenchward migration of forearc sedimentation. In addition, detrital zircon data from sedimentary rocks that underlie and intercalate with arc-related tholeiitic basalt in the Elmtree inlier (fig. 1) are presented in support of an unconformable relationship with underlying, Middle Ordovician ophiolitic rocks of the Devereaux Complex, supporting a genetic link with subduction of Tetagouche backarc oceanic lithosphere.

REGIONAL SETTING

Backarc Extension and Spreading: Bathurst and Fournier Supergroups

Tetagouche backarc crust comprises two distinct domains associated with progressive crustal extension and arc rifting: the Bathurst Supergroup represents the products of crustal extension and rifting of the Popelogan arc (continental domain), whereas the Fournier Supergroup represents the phase of oceanic lithosphere formation (oceanic domain). Each comprises three major thrust nappes that contain coeval, north-younging successions of volcanic and sedimentary rock. The Bathurst Supergroup consists of Floian to Katian volcanic and sedimentary rocks deposited during rifting and dismemberment of Ganderian continental crust, contemporaneous with Popelogan arc volcanism. The three major tectonostratigraphic subdivisions of the Bathurst Supergroup are, from structural top to bottom, the California Lake, Tetagouche and Sheephouse Brook groups (figs. 2 and 3). Each of these tectonostratigraphic units comprises late Floian – Darriwilian, dominantly felsic volcanic rocks, overlain by late Darriwilian – *ca.* mid Katian alkalic and mid-ocean ridge (MORB)-like basalt and deep marine sedimentary rocks (chert and shale) that are assigned to the Boucher Brook Formation (California Lake Group), Little River Formation (Tetagouche Group) and Slacks Lake Formation (Sheephouse Brook Group). The Boucher Brook Formation (California Lake Group) is locally overlain by siliciclastic turbidites of the Middle River Formation (new name), whereas the Little River Formation is overlain in the southeastern part of the Tetagouche Group by siliciclastic turbidites of the Tomogonops Formation and in the northern part by mixed calcareous and siliciclastic turbidites of the Melanson Brook Formation (new name) (figs. 2 and 3).

The newly erected, Darriwilian – Katian Fournier Supergroup (van Staal and Wilson, 2014) consists, from structurally highest to lowest, of the Devereaux (ophiolitic) Complex, the Pointe Verte Group, and Sormany Group (figs. 3 and 4). The tectonic contact between the Devereaux Complex and Pointe Verte Group is marked by a thin zone of *mélange* (fig. 5) that is locally structurally truncated, whereas the Pointe Verte and Sormany groups are juxtaposed along a thick and extensive belt of *mélange* (Belledune River *Mélange*; figs. 3 and 4). The Devereaux Complex comprises, in ascending order, the Black Point Gabbro (including minor pyroxenite and trondhjemite), the Belledune Point sheeted dikes, and pillow basalt of the Turgeon Road Formation. The Pointe Verte Group consists of the Prairie Brook Formation (a generally fining-upward succession of sedimentary rocks) and overlying Madran Formation (high-Cr alkalic pillow basalt). The Sormany Group is composed of the Armstrong Brook Formation (pillow basalt) and Millstream Formation (turbiditic wacke, fine-grained sedimentary rocks and limestone) in the northern part of the Miramichi inlier (figs. 2 and 3), and the Elmtree Formation (fine-grained sedimentary rocks) in the Elmtree inlier (figs. 3 and 4). Along the northern margin of the

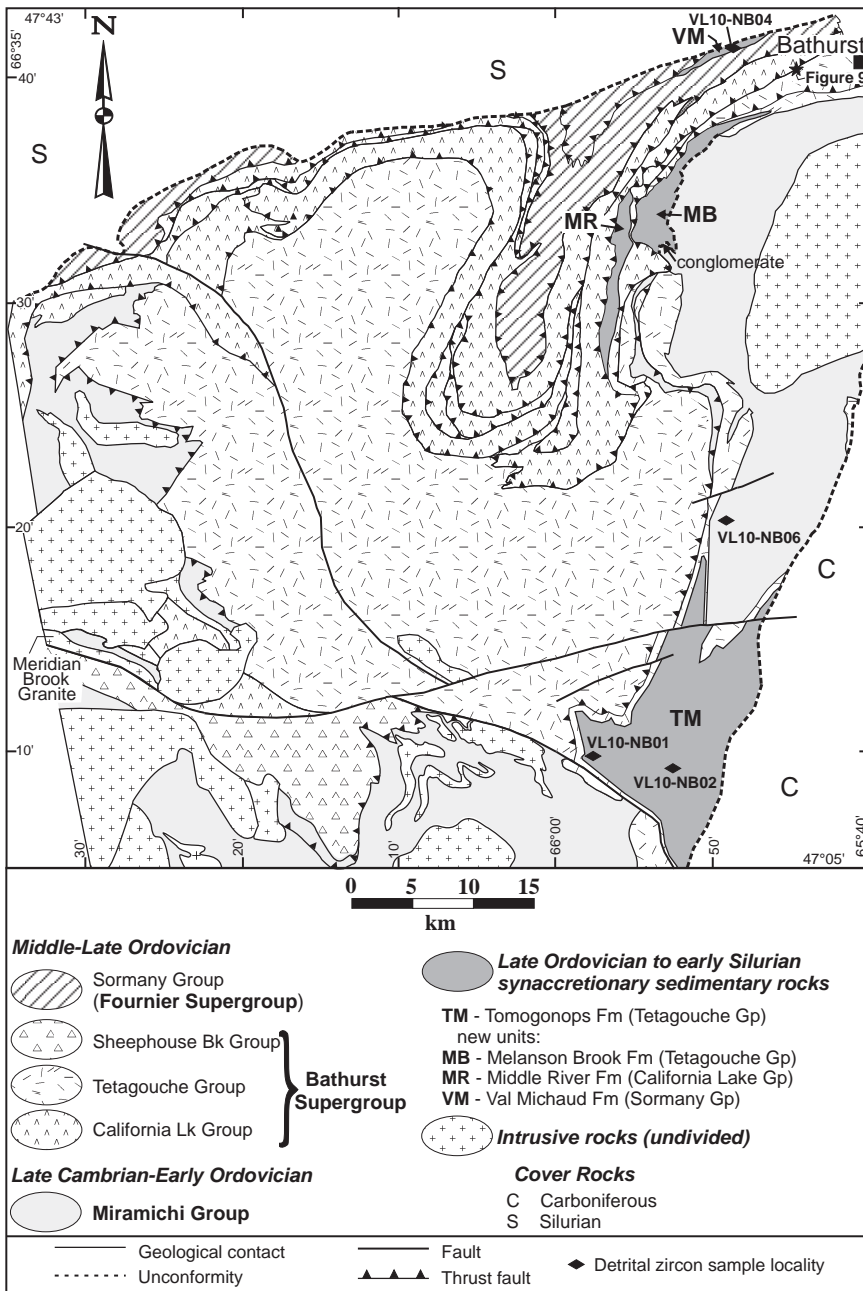


Fig. 2. Geological map of the Miramichi Highlands showing the distribution of major tectonostratigraphic elements (groups), the synaccretionary units discussed in this paper, and the location of samples collected for detrital zircon analysis. See figure 1 for location.

Miramichi inlier, the Millstream Formation is locally overlain by quartzofeldspathic sedimentary rocks of the Val Michaud Formation (new name; figs. 2 and 3). The Elmtree Formation, although consisting mainly of dark gray to black shale and

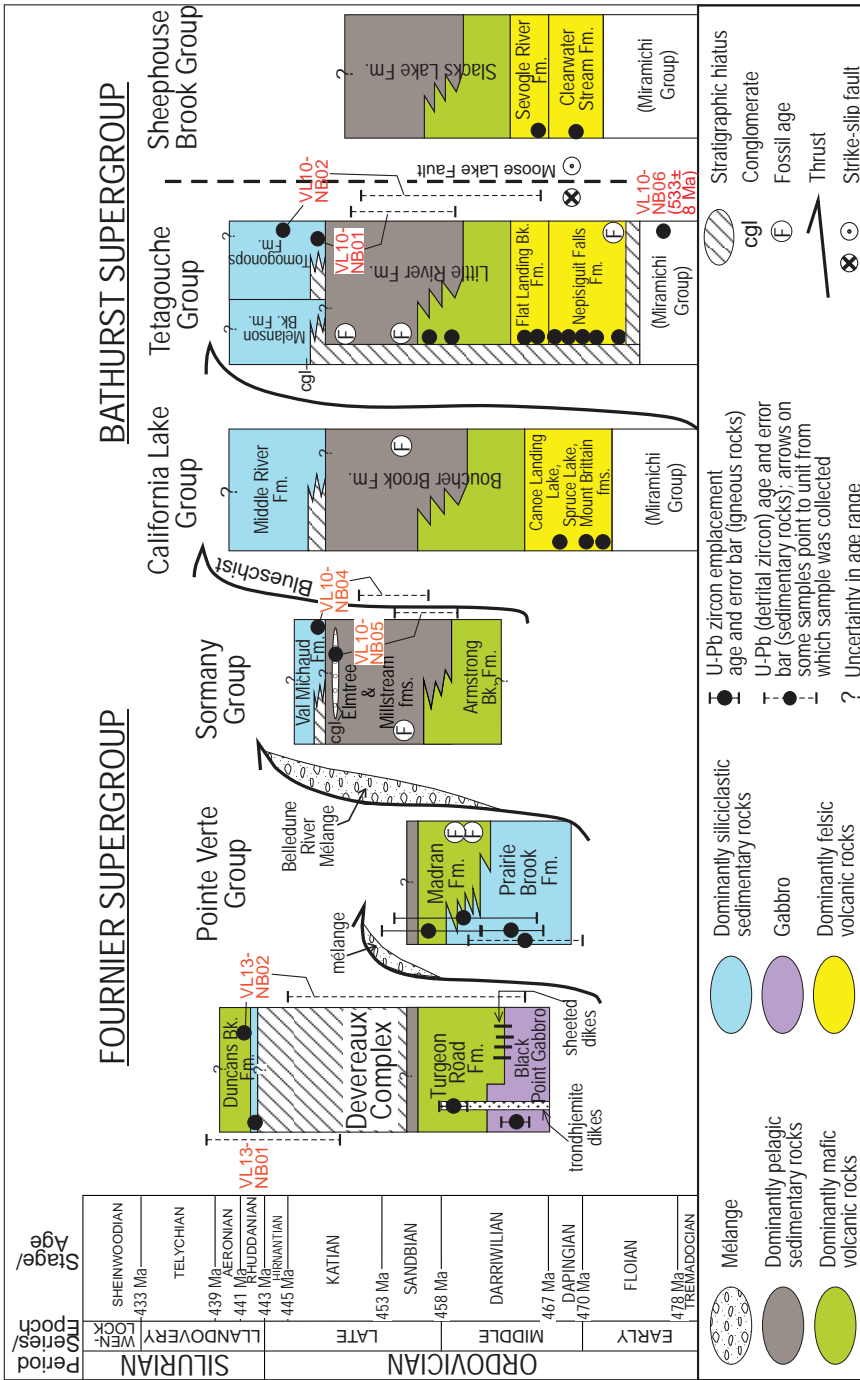


Fig. 3. Stratigraphic columns showing the tectonostratigraphic relationships between the various groups/nappes composing the Bathurst and Fournier supergroups. Detrital zircon sample numbers are shown in red font, and the age range of interpreted youngest populations are plotted as dashed lines beside the columns (see also figs. 13 and 14).

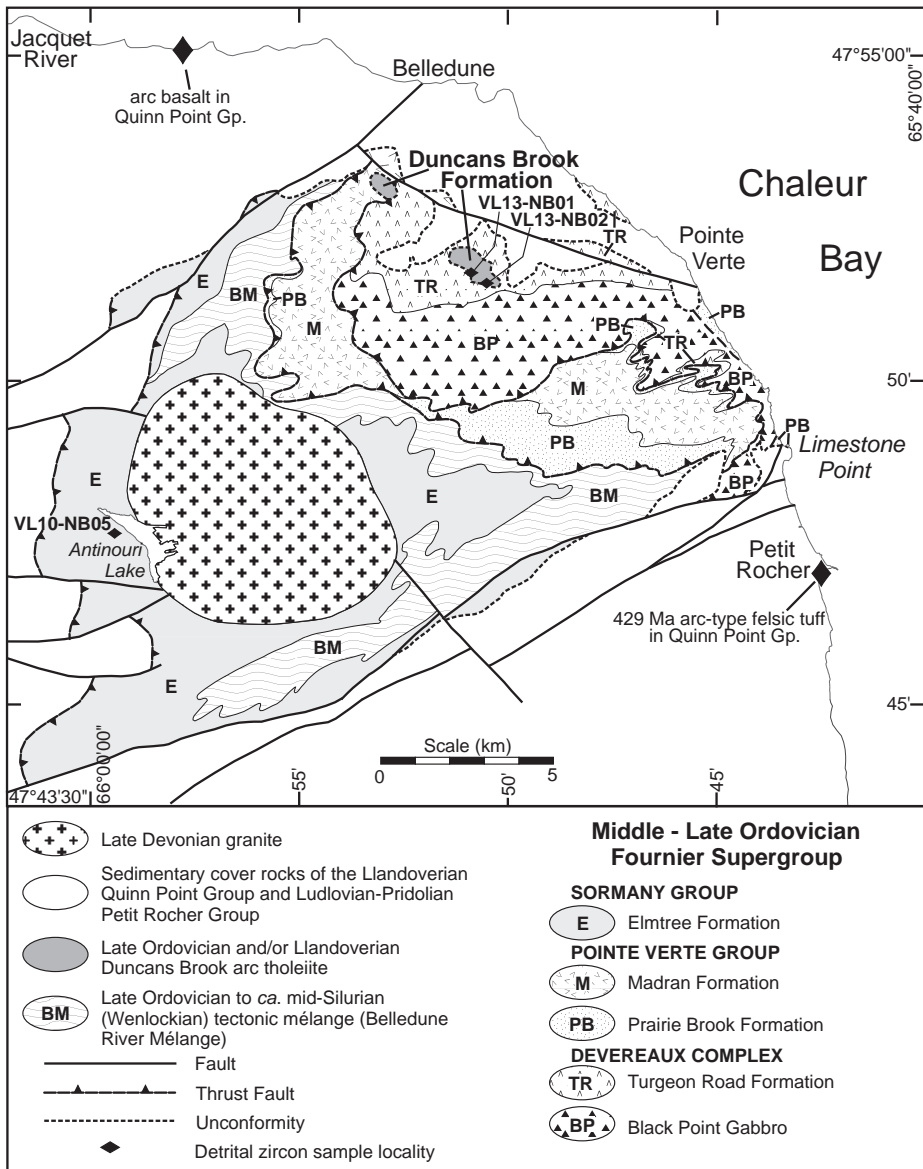


Fig. 4. Geological map of the Fournier Supergroup in the Elmtree inlier, showing location of samples collected for detrital zircon analysis, and subduction-related, Llandoverian – Wenlockian volcanic rocks of the Quinn Point Group (Wilson and others, 2008). See figure 1 for location.

siltstone, is locally (west of Antinour Lake; fig. 4) dominated by quartzose wacke containing minor pebbly conglomerate. Poor exposure prevents an understanding of the field relationship of these rocks to the dominant pelagic shale, hence a sample was collected for detrital zircon analysis to confirm a suspected younger age (see below).

Also in the Elmtree inlier, an areally restricted unit recognized by Winchester and others (1992) and referred to by them as the Duncans Brook arc tholeiite (figs. 3 and 4), is herein assigned formation status. The Duncans Brook Formation is spatially



Fig. 5. Tectonic mélange at the contact between the Devereaux Complex and Pointe Verte Group, Fournier Supergroup. The length of the hammer here and in subsequent photos is 40 cm.

associated with MORB-like basalt of the underlying Turgeon Road Formation, but its relationship with the Turgeon Road remained enigmatic until the recent discovery of a thin unit of quartz-rich sandstone and minor conglomerate between the two units, implying an unconformable relationship.

Forearc Sedimentation: The Matapedia Cover Sequence

The stratigraphic framework and evolution of the Matapedia cover sequence (MCS) in northern New Brunswick has been described by Wilson and others (2004). The MCS developed following the late Taconic collision of the Popelogan arc with Laurentia, and locally oversteps deformed Cambrian to Middle Ordovician rocks of the Humber and Notre Dame zones to the west, and Ganderia to the east (Malo and Bourque, 1993; van Staal and de Roo, 1995; fig. 1). Popelogan arc – Laurentia collision is recorded in western New Brunswick by an unconformity between the Middle Ordovician Craig Brook Formation (fig. 1) and Upper Ordovician rocks of the MCS (St. Peter, 1982; Fyffe and others, 2011), and in northern New Brunswick by a Late Ordovician disconformity between the MCS and underlying Darriwilian arc basalt and Sandbian chert of the Balmoral Group (Wilson, 2003; Wilson and others, 2004; fig. 1). Evidence that the Popelogan arc constitutes the substrate to the MCS consists of several major inliers of pre-Late Ordovician volcanic and sedimentary rocks in Maine, New Brunswick and the Gaspé Peninsula (van Staal and others, 2016) (fig. 1). In New Brunswick, the Notre Dame – Ganderia zone contact, corresponding to the Laurentia – Ganderia suture (Red Indian Line) is believed to occur at or near the trace of the Restigouche – Grand Pabos Fault (fig. 1), although the actual boundary is obscured by the cover rocks (Dupuis and others, 2009).

Post-Taconic closure of the Tetagouche backarc basin was achieved by northwest-directed subduction beneath the composite Laurentian margin, beginning *ca.* late Katian and terminating by early to middle Wenlockian (van Staal, 1994; van Staal and others, 2001, 2003, 2009). Arc magmatic activity related to Tetagouche backarc subduction is poorly represented in the northern Appalachians but includes Upper Ordovician to Llandoveryan volcanic rocks of the Quimby Formation in the Bronson Hill anticlinorium of New England (Tucker and Robinson, 1990; Moench and Aleinikoff, 2002), Llandoveryan intrusive and volcanic rocks in western Newfoundland (Whalen, 1989; Whalen and others, 2006), Llandoveryan volcanic and volcanoclastic



Fig. 6. (A) Interbedded fine-grained sandstone turbidites and mudstone hemipelagic deposits from the Boland Brook Formation (Grog Brook Group). (B) Parallel- and cross-laminated sandstone turbidite from the Whites Brook Formation (Grog Brook Group). Coin is 2.5 cm in diameter. (C) Thinly interbedded calcareous siltstone and calcilitite from the Pabos Formation (Matapedia Group). Compass is roughly 7×7 cm. (D) Thin-bedded calcilitite from the White Head Formation (Matapedia Group).

rocks of the Pointe aux Trembles and Lac Raymond formations in the western Gaspé Peninsula (David and Gariépy, 1990), and minor Llandoveryian to Wenlockian volcanic rocks of the Quinn Point Group in northeastern New Brunswick (Wilson and others, 2008; fig. 4). Because these magmatic rocks were dominantly emplaced in the orogenic hinterland farther west, Late Ordovician to Wenlockian sedimentary rocks of the MCS were deposited in the arc-trench gap (that is, a forearc setting) with respect to Tetagouche backarc subduction (van Staal and de Roo, 1995; Wilson and others, 2008).

Sedimentary rocks of the Matapedia forearc are preserved in the central belt of the MCS, namely the Aroostook – Percé Anticlinorium (fig. 1). The forearc succession comprises Upper Ordovician to Llandoveryian – Wenlockian turbidites, including (from base to top) a mid-late Katian siliciclastic assemblage (Grog Brook Group; figs. 6A and 6B), a Hirnantian to *ca.* late Aeronian deep-water carbonate mudstone assemblage (Matapedia Group; figs. 6C and 6D), and Aeronian to Telychian thin-bedded turbidites of the Quinn Point Group; together, these units represent a shallowing-upward, basin-fill succession that culminated with deposition of Telychian – Sheinwoodian shallow marine carbonates (Wilson and others, 2004). The latter are followed by a mid-Silurian hiatus (Salinic unconformity) recording uplift associated with the collision of the Popelogan arc (and its Ganderian substrate) with Laurentia (Wilson and Kamo, 2012; van Staal and others, 2016). Rocks of the MCS are correlated with Upper Ordovician to Silurian turbidites (graywacke, sandstone, shale and conglomerate) of the Badger Group in Newfoundland, which conformably overlie Katian black

shale of the Lawrence Harbour Formation (Williams and others, 1995; O'Brien, 2003; Waldron and others, 2012).

SYNACCRETIONARY SEDIMENTARY ROCKS OF THE BRUNSWICK SUBDUCTION COMPLEX

In the eastern and northern parts of the Miramichi Highlands (figs. 1 and 2), rocks that are lithologically similar to some of those that make up the forearc succession (Grog Brook and Matapedia groups) in the MCS are assigned to four formations, including three that are newly introduced herein. In the southeastern and northeastern parts of the Tetagouche Group, respectively, the Tomogonops Formation conformably to unconformably overlies and is locally in tectonic contact with the Little River Formation, and the Melanson Brook Formation conformably(?) to unconformably overlies the Little River Formation and unconformably overlies the Cambrian to Early Ordovician Miramichi Group (fig. 2). In the California Lake Group, the Middle River Formation overlies and is locally tectonically juxtaposed against the Boucher Brook Formation. In the Sormany Group, the Val Michaud Formation is locally in tectonic contact with the Millstream Formation, but elsewhere the nature of the contact is unclear. All these units are unfossiliferous (processing of numerous rock samples shows that microfossils are also absent), which may explain why lithological differences between them and underlying Sandbian – Katian pelagic shale were largely unappreciated in the past. However, several other criteria serve to distinguish these unfossiliferous rocks from the pelagic shale, including: 1) their dominantly quartzose or quartzofeldspathic composition; 2) their lighter color and coarser grain size; 3) their well-developed sedimentary structures and bedforms compared to the underlying rocks, in which such features are rare to absent; and 4) the calcareous nature of some units, especially the Melanson Brook Formation and parts of the Tomogonops Formation.

Tomogonops Formation (Tetagouche Group)

The name 'Tomogonops Formation' (fig. 2) was introduced by Langton (1993), although Dawson (1961) first recognized these rocks as a distinct mappable unit and placed them at the top of his Tetagouche Group. Similarly, Irrinki (1971) mapped "feldspathic and lithic graywackes, and locally calcareous laminated slate and phyllite" that he regarded as the upper part of the Tetagouche Group in this area. The Tomogonops Formation is lithologically diverse, but mainly consists of light to medium gray or greenish gray, fine- to medium-grained, thin- to medium-bedded, massive to laminated, locally calcareous quartz wacke, sandstone, slaty siltstone, and minor thicker-bedded (up to 1 m) feldspathic and lithic wacke and conglomerate. Sandstone locally displays sedimentary structures typical of deposition as turbidites, such as graded bedding, and parallel-, cross-, and convolute lamination (figs. 7A and 7B). In places, the unit is dominated by medium- to thick-bedded, feldspathic to arkosic wacke intercalated with dark gray, parallel-laminated mudstone.

Langton (1995) recognized a conformable contact between the Little River Formation and overlying Tomogonops Formation near sample location VL10-NB01 (fig. 2); similarly, near the northern limit of Tomogonops exposure, Walker (2005) concluded that the contact is gradational, placing the lower contact of the Tomogonops Formation at the base of the first calcareous bed. In contrast, recent examination by the principal author of core recovered during exploration drilling about 10 km northeast of VL10-NB01 revealed that the two units are tectonically juxtaposed at that location, supporting Langton's (1996) observation that the regional distribution of the Tomogonops Formation implies that locally the contact must be unconformable or tectonic.



Fig. 7. (A) Parallel- and cross-laminated turbidites from the Tomogonops Formation. (B) Thin-bedded sandstone turbidites of the Tomogonops Formation. (C) Thin-bedded calcilitite from the Melanson Brook Formation: compare with figure 6C from the Matapedia Group. (D) Thin-bedded to laminated, strongly calcareous slaty siltstone (calcisiltite) of the Melanson Brook Formation.

Melanson Brook Formation (Tetagouche Group)

The Melanson Brook Formation (fig. 2) consists mainly of dark gray or greenish gray, massive to prominently laminated, moderately to strongly calcareous, but locally non-calcareous slaty siltstone that grades to calcisiltite or calcilitite (carbonate mudstone; fig. 7C). Thin-bedded to laminated calcareous siltstone having a prominent S_{1-2} slaty cleavage is the dominant lithotype (fig. 7D), although local sandstone beds display graded bedding, cross-laminations and load casts demonstrating that at least part of the Melanson Brook consists of turbidites deposited in a relatively deep marine, slope environment. On its eastern margin, the Melanson Brook Formation unconformably overlies Lower Ordovician sedimentary rocks of the Patrick Brook Formation (Miramichi Group), and rounded pebbles and cobbles sourced from that unit locally form conglomerate beds at the base of the Melanson Brook (fig. 2). On the west, the contact with the California Lake Group is interpreted as tectonic, but the contact with underlying rocks of the Little River Formation (Tetagouche Group) may be in part tectonic and in part disconformable.

Designation of the Melanson Brook Formation as a distinct unit is made with caution, as these rocks occur in the same general area as calcareous mudstone and sandstone that lie at the base of the Tetagouche Group and disconformably overlie the Miramichi Group, namely the Vallée Lourdes Member of the Nepisiguit Falls Formation (Fyffe and others, 1997; van Staal and others, 2003). The thin Vallée Lourdes Member contains brachiopods (Fyffe, 1976) and conodonts (Nowlan, 1981) of Floian to Dapingian age; cross-bedding in calcarenitic sandstone and the local presence of

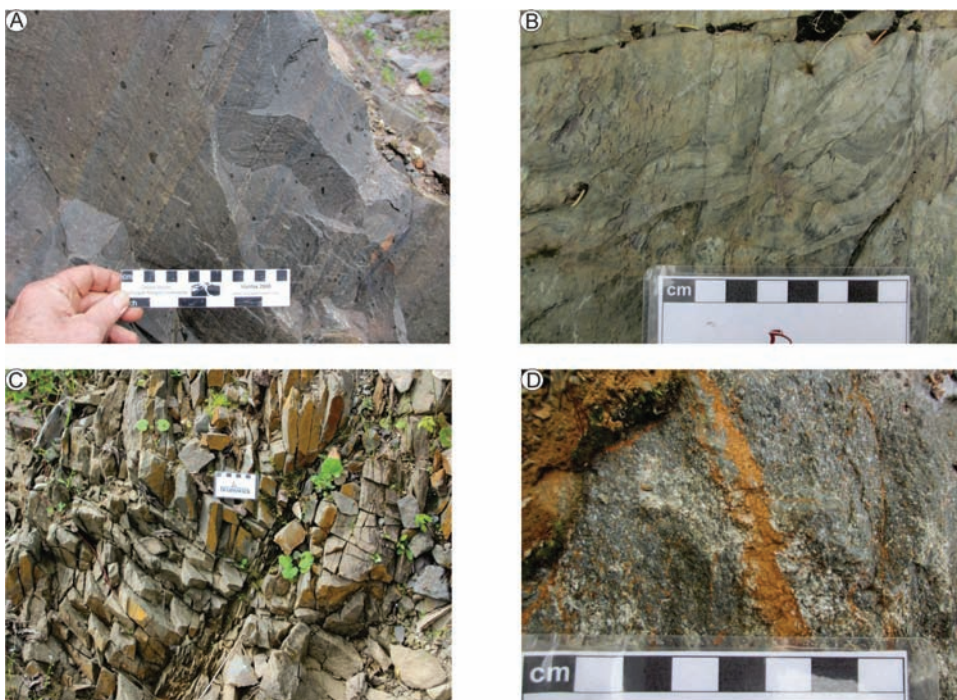


Fig. 8. (A) Thin-bedded turbidites exhibiting graded bedding and parallel lamination in the Middle River Formation. (B) Cross-laminated and convolute-laminated turbidite from the Middle River Formation. Compare these photos with figures 7A and 7B from the Tomogonops Formation. (C) Brown-weathered feldspathic sandstone from the Val Michaud Formation. (D) Coarse-grained, locally pebbly, quartzofeldspathic sandstone from the Val Michaud Formation.

cobble-boulder conglomerate suggests deposition in shallower water compared to the Melanson Brook Formation. In contrast, the latter occurs as a thick succession of unfossiliferous, typically thin-bedded to laminated calcareous mudstone and fine-grained sandstone (fig. 7D) hosting local sandy turbidite beds. Furthermore, the Melanson Brook belt truncates older rocks of the Tetagouche Group southwest of Bathurst (fig. 2); at its northern extremity, it pinches out within the Little River Formation, which it therefore appears to overlie disconformably. The abundance of dark gray calcilutite in the Melanson Brook invites comparison with poorly fossiliferous (in New Brunswick) carbonate mudstone turbidites of the White Head Formation in the Matapedia forearc basin (Ayrton and others, 1969; St. Peter, 1978; Malo, 1988).

Middle River Formation (California Lake Group)

The Middle River Formation (fig. 2) dominantly consists of medium to dark gray or greenish gray, typically prominently laminated but locally massive or cryptically laminated, non-calcareous slaty siltstone, along with varying proportions of light to medium gray, fine- to medium-grained, thin- to medium-bedded, non-calcareous, quartzose sandstone. Sedimentary structures such as graded beds, cross-bedding, load casts, and subtle to prominent bedding laminations are commonly developed in sandstone beds and indicate deposition as turbidites (figs. 8A and 8B). These features are much more common than in the Melanson Brook Formation, but the major distinction between the two units is the dominantly calcareous nature of the latter, versus the dominantly non-calcareous character of the Middle River Formation. The

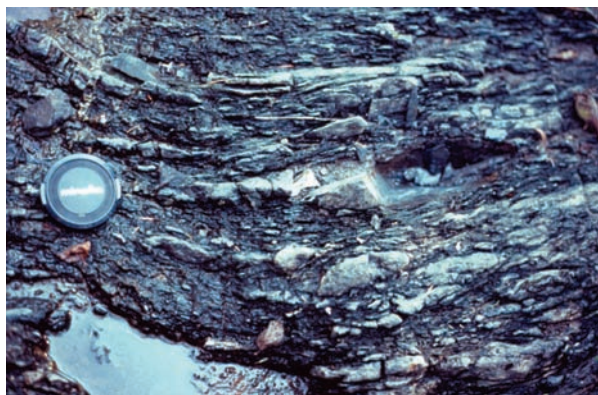


Fig. 9. Mélange containing Middle River-like sandstone clasts along the complex tectonic contact between the California Lake Group (Boucher Brook Formation) and the Tetagouche Group (Little River Formation). Lens cap is 5.5 cm in diameter. Location is along-strike from the main body of Middle River Formation (see fig. 2).

eastern contact of the Middle River Formation with the underlying Boucher Brook Formation has not been observed, but on the west, the Middle River is interpreted to be overthrust (west-to-east) by the Boucher Brook, based on several examples of tectonic *mélange* in the Boucher Brook Formation adjacent to the contact, including an isolated occurrence of *mélange* along strike to the northeast from the main body of Middle River Formation (fig. 9; location shown in fig. 2). The inferred easterly transport direction on this thrust is consistent with the interpreted vergence of thrust nappes and panels elsewhere in the Bathurst Supergroup (van Staal and de Roo, 1995; van Staal and others, 1988, 2001, 2003).

The lithotypes and sedimentary structures present in the Middle River Formation are very similar to those observed in the Tomogonops Formation (compare figs. 8A and 8B with figs. 7A and 7B), and to a lesser extent in the Melanson Brook Formation, although the abundant, medium to thick beds of feldspathic and lithic wacke seen in the Tomogonops are absent in both the Melanson Brook and Middle River formations. Turbidites that make up a large proportion of the Tomogonops and Middle River formations resemble lithofacies seen in the Grog Brook Group and suggest a linkage with the Matapedia forearc belt to the west (fig. 1).

Val Michaud Formation (Sormany Group)

The Val Michaud Formation is exposed in a small area in the extreme northern part of the Miramichi Highlands (fig. 2). The Val Michaud comprises light to medium gray or light grayish green, brown to pinkish-brown weathered, fine- to medium-grained quartzofeldspathic sandstone (fig. 8C), and subsidiary light gray or light green quartzose sandstone. Minor coarse- to very coarse-grained quartzofeldspathic sandstone (fig. 8D) and rare pebble conglomerate are also present. Outcrops are generally massive; bedding and sedimentary structures are rarely observed, suggesting that most beds are thick. The dominantly arenitic nature of the sedimentary rocks, presence of relatively clean quartz sandstone, and apparent roundness of at least the coarser grains, suggest reworking in a high-energy, proximal or relatively shallow marine environment, in contrast to the other synaccretionary units described above. On the northwestern boundary of the Val Michaud Formation, shearing in mudstone of the underlying Millstream Formation (fig. 3) implies that this contact is tectonic. Deformation in the Val Michaud Formation is weak and grade of metamorphism is low

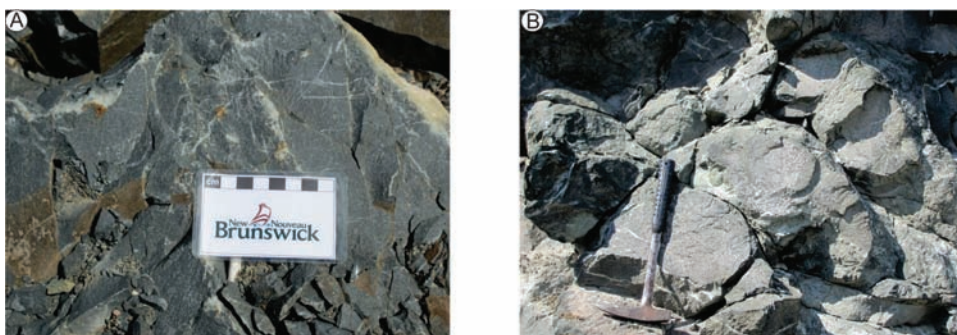


Fig. 10. (A) Quartzose sandstone from the base of the Duncans Brook Formation. (B) Pillow basalt from the Duncans Brook Formation.

(associated rocks are locally prehnite-bearing) compared to that seen in the other synaccretionary units, suggesting that these rocks remained at a relatively high structural level during deformation.

DUNCANS BROOK FORMATION: ARC VOLCANISM ASSOCIATED WITH TETAGOUCHE BACKARC SUBDUCTION

In the Elmtree inlier, Winchester and others (1992) recognized a distinctive suite of arc tholeiitic basalt they referred to as the Duncans Brook tholeiite (figs. 3 and 4). In view of the detrital zircon age of associated sedimentary rocks and the distinctive chemistry (see below) of the basalt, this unit is herein elevated to formation status and included in the Llandoveryan – Wenlockian Quinn Point Group. The type section of the Duncans Brook Formation is an aggregate quarry located south of Belledune and west of Pointe Verte (fig. 4); recent mapping and sampling have outlined the distribution of these rocks in more detail, including their occurrence in a second quarry farther to the northwest (fig. 4). The Duncans Brook Formation consists of a thin, discontinuous, basal unit of light gray, fine- to coarse-grained quartzose sandstone (fig. 10A) and conglomerate, and overlying light to medium green, massive to pillowed, Cr-rich, tholeiitic basalt (fig. 10B), minor associated hyaloclastite, and local interbedded red mudstone. The basal sandstone is very massive and rarely displays sedimentary structures or bedforms. In the south wall of the type-section quarry, basalt is juxtaposed against the sandstone along an apparent minor thrust, suggesting that the basalt is older. However, the distribution of sedimentary rocks to the south of the quarry, younging evidence from pillows, and sparse bedding attitudes, together imply that the sedimentary rocks underlie the Duncans Brook basalt and disconformably or unconformably overlie MORB-like pillowed flows (Winchester and others, 1992) of the late Darrivilian Turgeon Road Formation (Devereaux Complex). No upper contact is exposed.

Several samples of the Duncans Brook basalt were submitted for whole-rock geochemical analysis (table 1), to supplement the previously published data of Winchester and others (1992), and to compare with subduction-related basalt from the Llandoveryan Weir Formation (Wilson and others, 2008; fig. 4). The analytical facility, methods and procedures are the same as reported by Wilson and others (2008). The geochemistry of the Duncans Brook basalt (fig. 11; see also Winchester and others, 1992) points to possible affiliation with volcanic rocks of the Weir Formation; for example, discrimination diagrams normally used to infer tectonic setting (fig. 11) show that both groups display chemical signatures commonly seen in subduction-related basalt. However, the Duncans Brook basalt resembles arc tholeiitic lavas,

TABLE 1

Lithochemical analyses of tholeiitic basalt from the Duncans Brook Formation. Major oxides and S are reported as percentages and trace elements as parts per million

Sample #	RW14-TR5	RW14-TR9	RW14-TR10	RW14-TR11	RW14-TR12	RW14-TR23	RW14-TR30
SiO ₂	45.34	49.79	49.11	50.79	51.96	49.49	46.78
TiO ₂	0.58	0.48	0.43	0.55	0.54	0.44	0.45
Al ₂ O ₃	13.31	13.72	12.76	14.83	13.70	15.56	16.24
Fe ₂ O _{3t}	10.64	7.93	8.90	9.47	8.13	8.46	9.00
MnO	0.11	0.15	0.15	0.16	0.17	0.13	0.16
MgO	10.44	9.57	10.98	10.18	8.07	6.67	7.84
CaO	7.28	7.72	9.17	5.06	8.22	8.20	11.44
Na ₂ O	1.99	3.66	2.95	4.73	4.55	4.65	2.49
K ₂ O	2.05	0.98	0.67	0.28	0.67	0.56	0.06
P ₂ O ₅	0.10	0.06	0.05	0.08	0.08	0.06	0.05
LOI	6.60	5.61	4.08	4.73	4.17	5.83	4.96
TOTAL	98.47	99.68	99.25	100.90	100.30	100.00	99.48
Ba	332	167	246	179	370	126	54
Cr	242	425	641	465	360	89	113
Cs	1.9	0.4	0.5	0.4	0.2	2.0	0.6
Cu	182	84	92	39	57	125	146
Ga	15	12	11	12	12	16	15
Hf	1.1	0.8	0.7	1.0	1.0	0.9	0.6
Nb	3.9	5.1	2.8	3.5	3.8	1.7	6.0
Ni	108	153	183	218	139	46	79
Pb	2	2	2	2	3	2	4
Rb	36	15	11	5	10	8	2
S	0.584	0.121	0.115	0.073	0.090	0.160	0.091
Sc	36.0	38.0	45.0	40.0	38.0	39.0	41.0
Sr	210	158	86	101	104	185	192
Ta	0.08	0.19	0.05	0.15	0.16	0.09	0.01
Th	1.48	1.10	0.80	1.09	1.25	0.90	0.54
U	0.64	0.33	0.27	0.27	0.26	0.41	0.16
V	352	269	259	251	299	310	283
Y	15.9	11.2	10.7	15.8	14.7	13.1	10.5
Zn	48	58	60	64	55	55	56
Zr	38	28	21	34	33	29	19
La	10.80	5.21	4.22	7.71	8.16	4.80	3.68
Ce	23.30	11.50	9.09	15.70	16.20	10.00	8.09
Pr	2.89	1.43	1.21	2.00	2.02	1.29	1.12
Nd	11.90	6.23	5.40	8.88	8.76	5.81	5.38
Sm	2.69	1.58	1.45	2.18	2.07	1.44	1.43
Eu	0.81	0.39	0.41	0.75	0.70	0.51	0.51
Gd	2.74	1.81	1.72	2.63	2.44	1.86	1.62
Tb	0.46	0.32	0.31	0.44	0.43	0.36	0.29
Dy	2.82	2.09	1.91	2.82	2.65	2.35	1.90
Ho	0.58	0.45	0.40	0.61	0.56	0.52	0.41
Er	1.78	1.39	1.18	1.93	1.61	1.59	1.19
Tm	0.26	0.21	0.18	0.29	0.23	0.24	0.18
Yb	1.66	1.37	1.19	1.78	1.52	1.60	1.17
Lu	0.24	0.20	0.19	0.27	0.22	0.25	0.18

whereas the Weir basalt is calc-alkaline. Similarly, the Duncans Brook basalt has nearly flat rare-earth-element (REE) profiles (fig. 12A) and extended element patterns typical of island arc tholeiites (fig. 12B; Pearce, 1983), whereas the Weir basalt has

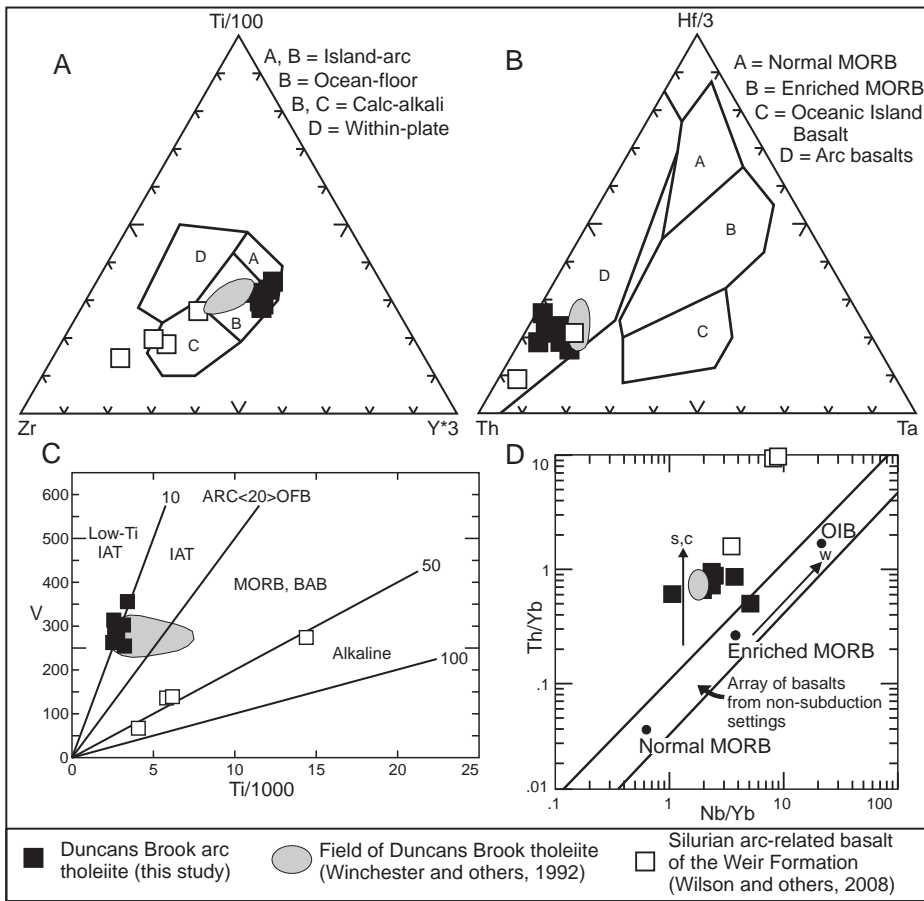


Fig. 11. Tectonic discrimination diagrams for basalt from the Duncans Brook and Weir formations. (A) Zr-Ti-Y diagram with fields defined by Pearce and Cann (1973); (B) Th-Hf-Ta diagram with fields defined by Wood and others (1979); (C) Ti vs. V diagram with fields defined by Shervais (1982); (D) Nb/Yb vs. Th/Yb diagram with fields defined by Pearce (2008). MORB – mid-ocean ridge basalt; IAT – island-arc tholeiite; OFB – ocean-floor basalt; BAB – back arc basin basalt; OIB – ocean island basalt; s, c – enrichments related to subduction and crustal contamination, respectively; w – within-plate enrichments.

sloping REE profiles and extended plots characteristic of calc-alkaline basalt erupted at active continental margins (fig. 12B).

GEOCHRONOLOGY

The Tomogonops, Middle River, Melanson Brook, and Val Michaud formations are barren of both macro- and microfossils and contain no interbedded volcanic rocks; hence they can only be dated indirectly. The age of the Tomogonops Formation is constrained by the underlying Little River Formation, which contains graptolites assigned to the Sandbian *Diplograptus multidentis* zone (Skinner, 1974; Langton, 1995). Similarly, the age of the Middle River Formation is constrained by the underlying Boucher Brook Formation, which contains conodonts assigned to the upper part of the Sandbian *Amorphognathus tvaerensis* zone (Skinner, 1974; Kennedy and others, 1979). No fossil ages are available for rocks underlying the Val Michaud or Duncans Brook formations. Detrital zircon analysis was therefore undertaken to establish

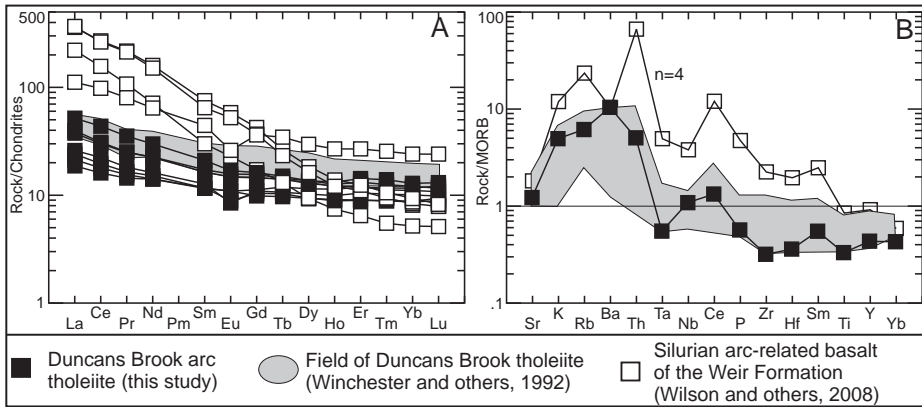


Fig. 12. (A) Chondrite-normalized rare-earth element profiles of basalt from the Duncans Brook and Weir formations. Normalizing values from Sun and McDonough (1989). (B) Mid-ocean ridge basalt-normalized extended element plot of average basalt compositions for the Duncans Brook and Weir formations. Normalizing values from Pearce (1983).

maximum depositional ages for the synaccretionary units discussed herein. Samples were collected from the Tomogonops Formation (VL10-NB01 and VL10-NB02), the Val Michaud Formation (VL10-NB04), the Elmtree Formation (VL10-NB05), and the Duncans Brook Formation (VL13-NB01 and VL13-NB02). In addition, micaceous sandstone from the Cambro-Ordovician Miramichi Group (VL10-NB06) was sampled so that the profile of detrital zircons available for recycling from older sedimentary rocks could be compared with those of the synaccretionary units. Sample descriptions and coordinates are given in table 2, and map locations are shown in figures 2 and 4. Probability density plots are illustrated in figures 13 and 14, and geochronologic data are presented in table 3. Data for samples VL10-NB01 and VL13-NB01 were reported by van Staal and others (2015); the probability density plots are included in figure 13 to allow easy comparison among all samples.

Heavy mineral separates were obtained by standard crushing, gravimetric and magnetic methods. Non-zircon components were hand-picked and removed from a representative aliquot of the heavy mineral separates. The remaining zircons were mounted in 2.54 cm epoxy rounds with natural zircon standards and polished to expose the grain interiors. Cathodoluminescence (CL) images were taken to character-

TABLE 2

Summary of samples collected for detrital zircon analysis

Sample #	Unit	Latitude	Longitude	Description
VL10-NB01	Tomogonops Fm.	47-09-57 N	65-57-23 W	Fine- to medium-grained sandstone
VL10-NB02	Tomogonops Fm.	47-09-38 N	65-52-45 W	Polymictic conglomerate
VL10-NB04	Val Michaud Fm.	47-41-26 N	65-49-24 W	Very coarse-grained quartzofeldspathic pebbly sandstone
VL10-NB05	Elmtree Fm.	47-47-34 N	65-59-07 W	Quartz pebble-rich quartzose wacke
VL13-NB01	Duncans Brook Fm.	47-51-41 N	65-50-42 W	Quartzose sandstone
VL13-NB02	Duncans Brook Fm.	47-51-37 N	65-50-23 W	Red mudstone
VL10-NB06	Knights Brook Fm.	47-20-54 N	65-48-06 W	Fine- to medium-grained micaceous sandstone

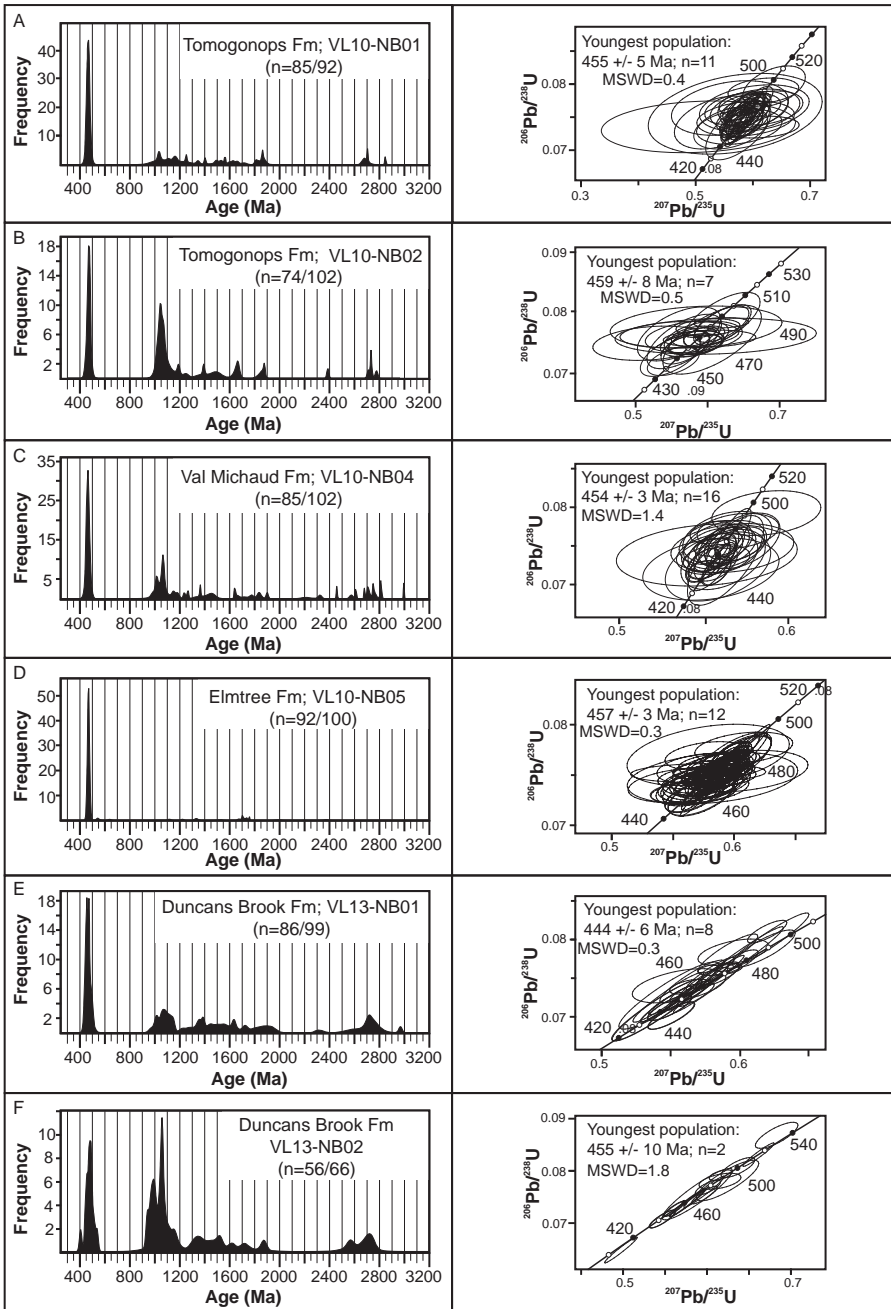


Fig. 13. Probability density plots of detrital zircon data and concordia plots of Paleozoic analyses from the (A, B) Tomogonops, (C) Val Michaud, (D) Elmtree, and (E, F) Duncans Brook formations. The youngest population ages were defined by the weighted mean of grains with $^{206}\text{Pb}/^{238}\text{U}$ ages that overlap at the 1σ level with $n \geq 2$ (Dickinson and Gehrels, 2009). Frequency noted on the vertical axis reflects histogram peak heights with 20-30 Ma bin width co-plotted with probability density plots. Plots and weighted mean ages with 2σ errors were generated by Isoplot (Ludwig, 2003).

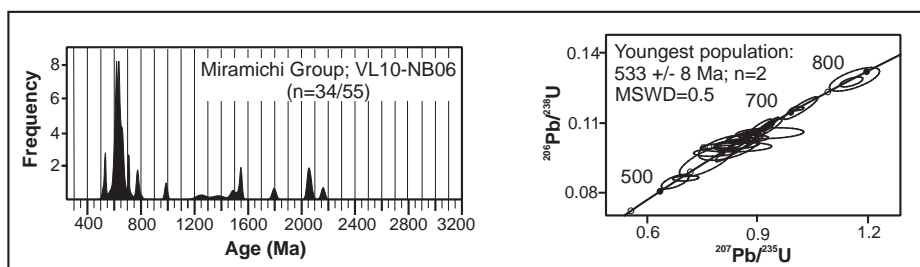


Fig. 14. Probability density plot for sample VL10-NB06 from the Miramichi Group. Frequency noted on the vertical axis reflects histogram peak heights with 25 Ma bin width co-plotted with probability density plot.

ize the internal structure and help place analytical spots in homogeneous domains within individual grains. U-Pb analysis was completed on a Nu Instruments HR ICPMS and New Wave UP193HE Excimer laser at the Arizona Laserchron Center following analytical methods of Gehrels and others (2006, 2008). U and Th concentrations and Pb/U fractionation were calibrated against the Arizona Laserchron Center Sri Lanka (SL) zircon standard (563.5 ± 3.2 Ma, 2σ ; ~ 518 ppm U and 68 ppm Th; Gehrels and others, 2008). Fractionation corrections were monitored by analysis of secondary zircon standard R33 (420.53 ± 0.16 Ma, 2σ ; Black and others, 2004; Mattinson, 2010). Common Pb corrections were made using ^{204}Hg -corrected ^{204}Pb measurements for each analysis and initial Pb compositions of Stacey and Kramers (1975). The $^{206}\text{Pb}/^{238}\text{U}$ ages are used for apparent ages less than 1200 Ma whereas $^{207}\text{Pb}/^{206}\text{Pb}$ ages are used for analyses greater than 1200 Ma. The age with lower uncertainty is used in cases where the $^{206}\text{Pb}/^{238}\text{U}$ and $^{207}\text{Pb}/^{206}\text{Pb}$ ages straddle 1200 Ma. Ages are excluded from discussion if (1) uncertainty of the best age is >10 percent at the 2σ level, (2) analyses >600 Ma are >10 percent discordant or >5 percent reversely discordant as determined by the difference between $^{206}\text{Pb}/^{238}\text{U}$ and $^{207}\text{Pb}/^{206}\text{Pb}$ ages without incorporating errors, or (3) analyses <600 Ma are discordant incorporating errors and thus avoiding exclusion due to difficulties in determination of $^{207}\text{Pb}/^{206}\text{Pb}$ ages for Paleozoic grains.

The youngest population of zircons used to define the maximum depositional age for each sample was defined by the weighted mean of $n \geq 2$ grains with $^{206}\text{Pb}/^{238}\text{U}$ ages that overlap at the 1σ level (Dickinson and Gehrels, 2009). Analyses used for calculation of maximum depositional age are noted by an asterisk in table 3. Samples from the Tomogonops and Val Michaud formations have nearly identical Sandbian ages of 455 ± 5 Ma, 459 ± 8 Ma, and 454 ± 3 Ma, indicating that the host rocks are late Sandbian or younger and likely overlap in age with the Grog Brook Group in the Matapedia forearc basin. The maximum depositional age of the Elmtree sample (457 ± 3 Ma) is nearly identical with those of the Tomogonops and Val Michaud formations (fig. 3), confirming that it most likely post-dates the *Nemagraptus gracilis* – lower *Diplograptus multidentis* age of graptolites recovered from Elmtree shale (McCutcheon and others, 1995). In the Duncans Brook Formation, the youngest populations of detrital zircons recovered from the basal quartzose sandstone (VL13-NB01) and from red mudstone intercalated with basalt (VL13-NB02) yield mean ages of 444 ± 6 Ma (\sim Ordovician – Silurian boundary) and 455 ± 10 Ma, respectively, implying that the basalt is latest Ordovician or possibly early Silurian.

The probability density plots for all the above samples are remarkably similar, although sample VL10-NB05 (Elmtree Formation) contains comparatively few grains older than Early Ordovician, and sample VL13-NB02 (Duncans Brook Formation) contains a much higher proportion of late Mesoproterozoic to early Neoproterozoic

TABLE 3
 LA-ICPMS U-Pb detrital zircon geochronologic data and apparent ages. * indicates data used in calculation of maximum depositional ages

Grain #	U (ppm)	²⁰⁶ Pb/ ²³⁸ U	²⁰⁷ Pb/ ²³⁵ U	Isotope ratios				Apparent ages (Ma)						Disc. (%)					
				²⁰⁶ Pb*/ ²³⁸ U	± (%)	²⁰⁷ Pb*/ ²³⁵ U*	± (%)	²⁰⁶ Pb*/ ²³⁸ U	± (Ma)	²⁰⁷ Pb*/ ²³⁵ U	± (Ma)	²⁰⁶ Pb*/ ²³⁸ U	± (Ma)		²⁰⁷ Pb*/ ²³⁵ U	± (Ma)			
82	224	31,624	0.6	17.9501	3.7	0.5515	4.3	0.0718	2.1	0.50	447	9	446	16	441	83	447	9	*
41	144	22,892	1.1	18.2906	4.0	0.5477	5.1	0.0727	3.0	0.60	452	13	443	18	399	91	452	13	*
37	323	110,396	0.9	17.9478	3.2	0.5684	4.0	0.0740	2.4	0.60	460	11	457	15	441	71	460	11	*
67	198	34,491	0.6	17.6449	4.0	0.5825	4.2	0.0745	1.5	0.34	463	7	466	16	479	88	463	7	*
50	197	28,396	0.6	17.8033	4.7	0.5778	5.1	0.0746	1.9	0.37	464	8	466	19	459	104	464	8	*
42	92	17,851	0.6	19.7408	9.9	0.5218	10.2	0.0747	2.4	0.24	464	11	426	36	225	230	464	11	*
10	200	40,051	0.6	18.2148	4.7	0.5677	6.0	0.0750	3.8	0.63	466	17	456	22	408	104	466	17	*
22	145	18,645	0.9	17.1177	5.7	0.6064	7.4	0.0753	4.8	0.65	468	22	481	29	546	124	468	22	*
96	157	1,631	0.7	17.2574	6.9	0.6028	7.0	0.0754	1.2	0.17	469	5	479	27	528	152	469	5	
85	160	37,909	0.7	17.8221	4.5	0.5845	5.0	0.0756	2.3	0.45	470	10	467	19	457	100	470	10	
47	129	37,260	0.6	17.9790	7.3	0.5810	7.7	0.0758	2.2	0.29	471	10	465	29	437	163	471	10	
81	245	7,249	1.0	16.1421	17.3	0.6473	17.5	0.0758	3.0	0.17	471	14	507	70	672	372	471	14	
55	227	15,234	0.8	17.5592	2.8	0.5952	3.2	0.0758	1.4	0.45	471	7	474	12	490	62	471	7	
59	69	7,312	1.2	17.1035	14.9	0.6114	15.1	0.0758	2.5	0.17	471	11	484	58	547	326	471	11	
31	233	24,236	0.6	17.9444	3.5	0.5828	3.7	0.0758	1.4	0.37	471	6	466	14	442	77	471	6	
16	77	10,000	0.7	18.6986	9.5	0.5611	9.7	0.0761	1.8	0.19	473	8	452	35	349	216	473	8	
58	75	7,027	0.6	18.7418	5.7	0.5605	6.8	0.0762	3.7	0.55	473	17	452	25	344	129	473	17	
19	360	82,828	0.7	17.8963	2.5	0.5885	2.6	0.0764	0.6	0.25	475	3	470	10	447	56	475	3	
33	223	32,007	0.5	17.7370	4.7	0.6006	4.9	0.0773	1.1	0.24	480	5	478	19	467	105	480	5	
27	122	55,260	0.5	18.2433	13.2	0.5841	13.5	0.0773	2.9	0.21	480	13	467	50	405	296	480	13	
1	90	55,815	0.6	17.2463	3.3	0.6206	4.2	0.0776	2.7	0.64	482	13	490	17	529	71	482	13	
48	189	38,393	0.2	17.2984	3.2	0.6197	4.0	0.0777	2.4	0.61	483	11	490	16	523	70	483	11	
5	176	19,971	0.8	17.3577	4.0	0.6192	4.0	0.0780	0.7	0.17	484	3	489	16	515	87	484	3	
36	199	22,009	0.5	17.4442	4.3	0.6197	5.7	0.0784	3.7	0.65	487	17	490	22	504	94	487	17	
60	184	816	0.4	13.8175	29.7	0.8627	29.9	0.0865	3.6	0.12	535	19	632	142	996	617	535	19	
99	46	14,532	0.6	13.8171	5.2	1.6703	5.7	0.1674	2.4	0.43	998	23	997	36	996	105	998	23	0
2	118	30,096	0.5	13.8840	2.6	1.6894	2.8	0.1701	1.2	0.42	1013	11	1005	18	987	52	1013	11	-3
34	77	27,073	0.2	13.5728	2.9	1.7360	3.6	0.1709	2.1	0.60	1017	20	1022	23	1033	58	1017	20	2
62	98	60,829	0.1	13.5693	4.2	1.7489	4.4	0.1721	1.2	0.27	1024	11	1027	28	1033	85	1024	11	1
57	83	30,771	0.4	13.4025	2.3	1.7813	3.0	0.1732	1.9	0.63	1029	18	1039	20	1058	47	1029	18	3
100	110	70,056	0.4	13.4128	1.9	1.7856	2.3	0.1737	1.2	0.53	1032	12	1040	15	1057	39	1032	12	2
15	174	91,147	0.1	13.4798	1.4	1.7789	2.1	0.1739	1.6	0.75	1034	15	1038	14	1047	28	1034	15	1

TABLE 3
(continued)

Grain #	U (ppm)	²⁰⁶ Pb/ ²⁰⁴ Pb	Th/U	Isotope ratios				Apparent ages (Ma)						Disc. (%)					
				²⁰⁶ Pb*/ ²⁰⁷ Pb*	\pm (%)	$\frac{^{206}\text{Pb}^*}{^{238}\text{U}}$	\pm (%)	$\frac{^{206}\text{Pb}^*}{^{235}\text{U}^*}$	error corr.	$\frac{^{206}\text{Pb}^*}{^{235}\text{U}^*}$	\pm (Ma)	$\frac{^{207}\text{Pb}^*}{^{235}\text{U}}$	\pm (Ma)		$\frac{^{206}\text{Pb}^*}{^{207}\text{Pb}^*}$	\pm (Ma)	Best age (Ma)	\pm (Ma)	
83	73	15,637	0.3	13.7525	5.1	1.7491	5.1	0.1745	1.0	0.19	1037	9	1027	33	1006	103	1037	9	-3
13	138	58,338	0.3	13.5867	2.3	1.7822	2.5	0.1756	0.8	0.33	1043	8	1039	16	1031	47	1043	8	-1
93	67	30,600	0.7	13.1890	5.0	1.8379	5.1	0.1758	1.4	0.27	1044	13	1059	34	1090	99	1044	13	4
61	67	30,257	0.3	13.5032	2.9	1.7995	3.3	0.1762	1.7	0.50	1046	16	1045	22	1043	59	1046	16	0
14	125	60,700	0.5	13.4720	2.0	1.8077	2.4	0.1766	1.3	0.53	1049	12	1048	16	1048	41	1049	12	0
23	152	88,299	0.2	13.4656	1.7	1.8110	1.9	0.1769	0.9	0.46	1050	8	1049	12	1049	34	1050	8	0
21	56	13,557	0.5	13.5261	7.0	1.8104	7.2	0.1776	1.4	0.19	1054	13	1049	47	1040	142	1054	13	-1
20	67	22,615	0.3	12.9262	3.0	1.8957	3.2	0.1777	1.1	0.34	1055	11	1080	21	1131	60	1055	11	7
25	86	30,418	0.3	13.0822	2.9	1.8852	4.6	0.1789	3.6	0.78	1061	35	1076	31	1107	58	1061	35	4
89	121	38,465	0.3	13.6565	1.5	1.8078	1.9	0.1791	1.2	0.60	1062	11	1048	13	1020	31	1062	11	-4
40	83	31,215	0.8	13.4836	2.7	1.8446	3.5	0.1804	2.1	0.61	1069	21	1062	23	1046	55	1069	21	-2
52	163	77,409	0.8	13.2493	1.8	1.8777	3.2	0.1807	2.6	0.82	1069	26	1073	21	1081	36	1069	26	1
72	413	209,827	0.3	13.2203	1.1	1.8846	1.3	0.1807	0.7	0.52	1071	6	1076	8	1086	22	1071	6	1
95	163	44,681	0.4	13.2371	1.6	1.8844	2.6	0.1809	2.1	0.81	1072	21	1076	17	1083	31	1072	21	1
6	174	37,572	0.4	13.2894	1.3	1.8815	2.5	0.1813	2.2	0.85	1074	21	1075	17	1075	27	1074	21	0
66	166	75,768	0.6	13.1988	1.4	1.8960	1.8	0.1815	1.0	0.59	1075	10	1080	12	1089	29	1075	10	1
43	71	28,903	0.5	13.3394	3.2	1.8927	3.5	0.1831	1.3	0.38	1084	13	1079	23	1068	65	1084	13	-2
84	216	100,746	0.2	13.1217	0.6	1.9470	2.7	0.1853	2.6	0.97	1096	26	1097	18	1101	13	1096	26	0
80	188	68,817	0.3	12.9885	1.7	1.9943	2.4	0.1879	1.7	0.72	1110	18	1114	16	1121	33	1110	18	1
94	19	12,100	0.9	13.2875	9.9	1.9625	10.8	0.1891	4.3	0.40	1117	44	1103	73	1075	199	1117	44	-4
76	150	175,606	0.3	13.0107	2.0	2.0395	3.0	0.1924	2.3	0.76	1135	24	1129	21	1118	39	1135	24	-2
46	36	15,187	0.4	12.8780	5.3	2.1467	5.9	0.2005	2.6	0.44	1178	28	1164	41	1138	105	1178	28	-4
18	341	180,334	0.7	12.5858	0.6	2.2214	1.1	0.2028	0.9	0.81	1190	9	1188	7	1184	12	1190	9	-1
35	17	7,116	0.4	12.1955	7.6	2.2953	8.2	0.2030	3.1	0.37	1192	33	1211	58	1245	149	1192	33	4
7	105	74,871	0.7	12.1554	1.0	2.5608	2.9	0.2258	2.7	0.94	1312	33	1290	21	1252	20	1252	20	-5
54	92	25,451	0.3	11.4982	2.3	2.9478	2.6	0.2458	1.1	0.42	1417	14	1394	19	1360	45	1360	45	-4
24	55	28,808	0.2	11.3467	3.3	2.9313	4.7	0.2412	3.3	0.71	1393	42	1390	36	1385	64	1385	64	-1
56	390	234,645	0.3	11.3086	0.4	2.9226	0.8	0.2397	0.7	0.86	1385	8	1388	6	1392	8	1392	8	0
70	50	25,398	0.8	11.1539	2.3	2.9927	2.8	0.2421	1.6	0.58	1398	20	1406	21	1418	43	1418	43	1
69	93	24,265	0.9	10.8080	1.5	3.2933	2.4	0.2581	1.9	0.79	1480	25	1479	19	1478	28	1478	28	0
30	110	59,460	0.4	10.6047	1.7	3.1279	6.3	0.2406	6.1	0.96	1390	77	1440	49	1514	32	1514	32	8
32	55	60,315	0.7	10.5770	2.8	3.4402	3.6	0.2639	2.3	0.63	1510	30	1514	28	1519	53	1519	53	1

TABLE 3
(continued)

Grain #	U (ppm)	²⁰⁶ Pb/ ²⁰⁴ Pb	Th/U	Isotope ratios				Apparent ages (Ma)						Disc. (%)					
				²⁰⁶ Pb*/ ²⁰⁷ Pb*	\pm (%)	²⁰⁷ Pb*/ ²³⁵ U*	\pm (%)	²⁰⁶ Pb*/ ²³⁸ U*	\pm (Ma)	²⁰⁷ Pb*/ ²³⁵ U	\pm (Ma)	²⁰⁶ Pb*	\pm (Ma)		Best age (Ma)	\pm (Ma)			
VL10NB02 (n=76/102)																			
97	139	90,496	0.6	9.9463	1.0	3.9557	2.3	0.2854	2.1	0.90	1618	30	1625	19	1634	18	1634	18	1
74	111	158,153	0.7	9.8326	0.8	4.1684	2.3	0.2973	2.2	0.93	1678	32	1668	19	1655	15	1655	15	-1
8	345	177,975	0.1	9.7840	0.6	3.7872	1.7	0.2687	1.6	0.94	1534	21	1590	13	1665	10	1665	10	8
11	291	9,007	1.0	9.7340	0.8	4.1203	1.5	0.2909	1.2	0.85	1646	18	1658	12	1674	14	1674	14	2
38	74	61,865	0.1	8.8975	1.2	5.1371	1.5	0.3315	0.9	0.61	1846	15	1842	13	1838	22	1838	22	0
12	192	14,405	0.3	8.7744	0.8	5.3331	2.5	0.3394	2.4	0.95	1884	38	1874	21	1864	14	1864	14	-1
78	268	196,615	0.3	8.7026	0.4	5.3091	0.8	0.3351	0.7	0.87	1863	11	1870	7	1878	7	1878	7	1
39	162	157,585	1.0	6.5117	0.5	9.5356	0.9	0.4503	0.8	0.85	2397	15	2391	8	2386	8	2386	8	0
65	98	174,626	0.7	5.3643	0.6	13.3765	1.1	0.5204	0.9	0.86	2701	21	2707	10	2711	9	2711	9	0
17	289	138,438	0.6	5.3008	0.2	13.8438	1.4	0.5322	1.4	0.99	2751	31	2739	13	2730	4	2730	4	-1
51	87	99,572	1.5	5.2796	0.4	13.8958	0.7	0.5321	0.5	0.78	2750	11	2743	6	2737	7	2737	7	0
4	98	113,678	0.4	5.1552	0.6	14.1637	2.9	0.5296	2.9	0.98	2740	64	2761	28	2776	10	2776	10	1
Rejected Analyses (>10% discordance, >5% reverse discordance, or >10% 2s age uncertainty)																			
92	383	81,815	0.7	17.7099	1.2	0.5551	5.3	0.0713	5.2	0.98	444	22	448	19	471	26	471	26	
63	61	733	0.4	18.4179	11.6	0.5478	13.5	0.0732	7.0	0.52	455	31	444	49	383	261	383	261	
53	253	170	0.8	11.9155	18.8	0.8566	19.9	0.0740	6.3	0.32	460	28	628	93	1291	370	1291	370	
64	162	34,652	0.4	9.0887	21.0	1.1339	27.8	0.0747	18.1	0.65	465	81	770	151	1800	387	1800	387	
77	344	2,756	0.3	15.5741	3.8	0.8217	5.0	0.0928	3.3	0.65	572	18	609	23	749	81	749	81	
86	438	76,732	0.1	15.5906	2.0	0.8416	2.2	0.0952	1.0	0.46	586	6	620	10	746	41	746	41	
29	223	1,494	0.7	12.1886	11.5	1.7565	11.8	0.1553	2.6	0.22	930	23	1030	77	1247	226	1247	226	
87	34	8,252	0.9	14.8173	8.1	1.5274	8.6	0.1641	2.7	0.32	980	25	941	53	853	169	853	169	
75	51	23,034	1.2	14.2240	4.7	1.6189	4.9	0.1670	1.4	0.29	996	13	978	31	937	97	937	97	
90	21	8,053	0.6	13.9724	12.3	1.6968	13.0	0.1720	4.2	0.32	1023	39	1007	83	974	252	974	252	
91	10	3,512	0.9	13.6799	24.1	1.7374	27.1	0.1724	12.3	0.46	1025	117	1023	176	1017	495	1017	495	
49	73	33,727	1.2	13.9823	2.8	1.7002	3.2	0.1724	1.7	0.53	1025	16	1009	21	972	56	972	56	
9	68	43,290	0.2	14.1440	3.9	1.7102	4.2	0.1754	1.4	0.34	1042	14	1012	27	949	80	949	80	
44	28	21,634	1.3	13.7226	10.0	1.7814	10.2	0.1773	1.8	0.18	1052	17	1039	66	1010	204	1010	204	
3	42	28,068	0.8	14.3517	6.8	1.7278	7.0	0.1798	1.5	0.22	1066	15	1019	45	919	140	919	140	
28	28	11,747	0.6	15.2319	11.6	1.6308	11.9	0.1802	3.0	0.25	1068	29	982	75	795	243	795	243	

TABLE 3
(continued)

Grain #	U (ppm)	$\frac{^{206}\text{Pb}}{^{204}\text{Pb}}$	$\frac{\text{Th}}{\text{U}}$	Isotope ratios				Apparent ages (Ma)				Disc. (%)							
				$\frac{^{206}\text{Pb}^*}{^{207}\text{Pb}^*}$	\pm (%)	$\frac{^{207}\text{Pb}^*}{^{235}\text{U}^*}$	\pm (%)	$\frac{^{206}\text{Pb}^*}{^{238}\text{U}^*}$	\pm (Ma)	$\frac{^{207}\text{Pb}^*}{^{235}\text{U}^*}$	\pm (Ma)		Best age \pm (Ma)						
VLI0NB02 (n=76/102)																			
<i>Rejected Analyses (>10% discordance, >5% reverse discordance, or >10% 2s age uncertainty)</i>																			
79	152	37,369	0.5	13.3607	3.0	1.9041	6.5	0.1845	5.8	0.89	1092	58	1083	43	1064	61			
26	167	70,340	0.2	9.6207	3.6	2.6460	7.6	0.1846	6.8	0.88	1092	68	1314	56	1696	66			
98	72	27,210	0.7	13.5908	3.2	1.9376	8.1	0.1910	7.5	0.92	1127	77	1094	55	1030	64			
68	61	4,766	0.5	12.5408	5.6	2.1816	9.3	0.1984	7.5	0.80	1167	80	1175	65	1191	110			
73	86	11,322	0.4	10.1126	7.4	3.2196	8.4	0.2361	3.8	0.46	1367	47	1462	65	1603	139			
88	22	11,994	0.4	10.5316	29.6	3.5986	52.7	0.2749	43.6	0.83	1565	608	1549	445	1527	570			
45	84	65,180	0.7	9.9256	0.9	4.3058	1.4	0.3100	1.0	0.72	1741	15	1694	11	1638	17			
71	88	70,489	0.4	5.5294	0.6	10.8683	2.7	0.4359	2.6	0.97	2332	51	2512	25	2661	10			
VLI0NB04 (n=85/101)																			
36	165	28,556	0.8	17.3860	2.4	0.5698	3.0	0.0719	1.7	0.58	447	7	458	11	511	53			*
51	164	20,276	0.8	18.1336	3.2	0.5473	3.3	0.0720	1.1	0.32	448	5	443	12	418	70			*
15	59	14,844	0.9	17.7516	13.7	0.5595	14.2	0.0720	3.7	0.26	448	16	451	52	466	306			*
44	90	17,816	0.6	17.4587	10.0	0.5716	10.8	0.0724	4.1	0.38	450	18	459	40	502	220			*
35	167	16,806	0.9	18.3196	3.1	0.5462	3.7	0.0726	2.0	0.53	452	9	442	13	395	70			*
2	175	31,240	0.8	17.6499	3.9	0.5692	4.4	0.0729	2.1	0.47	453	9	458	16	478	87			*
33	173	28,802	0.6	17.2132	5.5	0.5864	7.6	0.0732	5.2	0.68	455	23	469	28	533	121			*
39	49	33,219	0.8	17.3659	7.7	0.5822	8.5	0.0733	3.5	0.41	456	15	466	32	514	170			*
57	153	17,755	0.9	17.9185	3.8	0.5649	5.3	0.0734	3.7	0.70	457	16	455	19	445	84			*
76	151	7,698	0.7	17.7541	6.7	0.5704	6.9	0.0734	1.6	0.24	457	7	458	25	465	148			*
21	244	59,623	0.7	17.4693	2.0	0.5797	2.7	0.0735	1.9	0.69	457	8	464	10	501	43			*
38	524	92,985	0.7	17.4997	1.1	0.5804	1.8	0.0737	1.4	0.77	458	6	465	7	497	25			*
93	58	30,700	1.4	18.4141	18.8	0.5534	19.1	0.0739	3.6	0.19	460	16	447	69	384	426			*
24	164	30,414	0.8	18.1376	3.3	0.5621	3.8	0.0739	1.9	0.50	460	8	453	14	418	73			*
30	126	27,435	0.9	17.8637	8.0	0.5717	8.3	0.0741	2.4	0.28	461	11	459	31	452	177			*
61	106	11,191	0.5	18.1733	4.6	0.5631	5.1	0.0742	2.2	0.42	462	10	454	19	413	103			*
69	341	56,715	0.8	17.7280	2.3	0.5788	3.0	0.0744	1.9	0.63	463	8	464	11	468	51			*
89	80	17,506	1.1	18.2678	5.9	0.5627	6.4	0.0746	2.4	0.38	464	11	453	23	402	132			*
18	273	61,168	0.8	17.9780	1.9	0.5718	2.4	0.0746	1.5	0.62	464	7	459	9	437	42			*

TABLE 3
(continued)

Grain #	U (ppm)	$\frac{^{206}\text{Pb}}{^{238}\text{U}}$	Th/U	Isotope ratios				Apparent ages (Ma)						Disc. (%)				
				$\frac{^{206}\text{Pb}^*}{^{207}\text{Pb}^*}$	\pm	$\frac{^{207}\text{Pb}^*}{^{235}\text{U}^*}$	\pm	$\frac{^{206}\text{Pb}^*}{^{238}\text{U}^*}$	\pm	error corr.	$\frac{^{206}\text{Pb}^*}{^{238}\text{U}^*}$	\pm	$\frac{^{207}\text{Pb}^*}{^{235}\text{U}^*}$		\pm	$\frac{^{206}\text{Pb}^*}{^{207}\text{Pb}^*}$	\pm	Best age (Ma)
VL10NB04 (n=85/101)																		
92	81	25,651	0.8	17,2299	11.7	0.5986	12.0	0.0748	2.8	0.23	465	12	476	46	531	257	465	12
88	190	24,566	0.7	18,1390	4.3	0.5691	4.5	0.0749	1.0	0.22	465	4	457	16	417	97	465	4
27	83	18,162	0.8	17,6256	5.6	0.5867	6.0	0.0750	2.2	0.37	466	10	469	23	481	124	466	10
13	100	17,989	1.0	17,7380	4.5	0.5840	5.1	0.0751	2.3	0.46	467	11	467	19	467	100	467	11
70	45	6,208	0.5	17,7105	7.8	0.5856	8.3	0.0752	2.7	0.33	468	12	468	31	471	174	468	12
90	199	4,118	0.8	16,9934	4.4	0.6114	4.8	0.0754	1.9	0.40	468	9	484	18	561	95	468	9
45	183	40,030	0.5	17,7009	3.2	0.5878	3.7	0.0755	1.8	0.49	469	8	469	14	472	71	469	8
16	98	18,573	0.9	18,2943	7.1	0.5693	7.5	0.0755	2.5	0.33	469	11	458	28	398	160	469	11
55	76	32,641	1.3	16,9494	6.5	0.6160	7.2	0.0757	3.1	0.43	471	14	487	28	567	141	471	14
19	97	3,596	0.8	17,8009	8.4	0.5897	8.9	0.0761	2.9	0.33	473	13	471	33	459	186	473	13
28	231	40,357	0.8	17,6043	2.1	0.6002	3.5	0.0766	2.8	0.80	476	13	477	13	484	46	476	13
47	102	16,727	0.7	18,8299	4.4	0.5624	4.6	0.0768	1.2	0.27	477	6	453	17	333	99	477	6
53	109	15,145	0.8	17,4450	7.6	0.6086	7.9	0.0770	1.9	0.24	478	9	483	30	504	168	478	9
11	69	8,992	1.0	16,5955	9.4	0.6588	9.7	0.0793	2.4	0.25	492	11	514	39	613	203	492	11
12	19	7,794	3.0	13,5939	11.9	1.6894	12.5	0.1666	3.7	0.30	993	34	1005	80	1029	242	993	34
7	176	24,912	1.5	13,3168	1.2	1.7338	7.2	0.1675	7.1	0.99	998	66	1021	47	1071	24	998	66
64	129	133,835	0.4	13,7559	2.4	1.6546	2.8	0.1651	1.4	0.49	985	12	991	18	1005	49	985	12
59	158	123,815	0.3	13,5832	1.5	1.7268	1.8	0.1701	1.1	0.60	1013	10	1019	12	1031	30	1013	10
41	147	55,949	0.9	13,4085	1.4	1.7602	1.9	0.1712	1.3	0.67	1019	12	1031	12	1057	29	1019	12
96	84	51,701	0.7	13,6331	2.9	1.7368	3.2	0.1717	1.4	0.44	1022	13	1022	20	1024	58	1022	13
77	103	69,244	0.6	13,5003	3.3	1.7368	3.5	0.1701	0.9	0.25	1012	8	1022	22	1043	67	1012	8
42	41	16,815	0.9	13,4923	4.9	1.7923	5.2	0.1754	1.8	0.34	1042	17	1043	34	1045	99	1042	17
3	101	37,137	1.0	13,4834	3.0	1.8224	3.4	0.1782	1.6	0.47	1057	16	1054	22	1046	60	1057	16
68	463	207,172	0.0	12,9940	0.4	1.8798	1.9	0.1772	1.9	0.98	1051	18	1074	13	1120	7	1051	18
54	168	51,769	0.4	13,3576	1.3	1.8420	2.4	0.1785	2.0	0.84	1059	20	1061	16	1065	27	1059	20
81	147	115,894	0.4	13,2025	0.9	1.8756	1.4	0.1796	1.1	0.77	1065	11	1073	9	1088	18	1065	11
80	194	100,512	1.3	13,3198	1.2	1.8613	1.4	0.1798	0.8	0.52	1066	7	1067	10	1071	25	1066	7
75	85	35,252	0.5	13,3182	2.4	1.8636	2.6	0.1800	0.8	0.33	1067	8	1068	17	1071	49	1067	8
62	389	168,839	0.1	12,9293	0.4	1.9235	1.9	0.1804	1.8	0.97	1069	18	1089	13	1130	9	1069	18
8	45	15,906	0.6	12,9760	2.5	1.9197	2.8	0.1807	1.3	0.47	1071	13	1088	19	1123	50	1071	13
4	586	278,585	0.1	13,3190	0.8	1.8778	2.1	0.1814	2.0	0.93	1075	20	1073	14	1071	16	1075	20

TABLE 3
(continued)

Grain #	U (ppm)	$\frac{^{206}\text{Pb}}{^{204}\text{Pb}}$	Th/U	Isotope ratios				Apparent ages (Ma)				Disc. (%)							
				$\frac{^{206}\text{Pb}^*}{^{207}\text{Pb}^*}$	\pm (%)	$\frac{^{206}\text{Pb}^*}{^{238}\text{U}}$	\pm (%)	$\frac{^{206}\text{Pb}^*}{^{238}\text{U}^*}$	error corr.	$\frac{^{206}\text{Pb}^*}{^{238}\text{U}^*}$	\pm (Ma)		$\frac{^{206}\text{Pb}^*}{^{207}\text{Pb}^*}$	\pm (Ma)	Best age \pm (Ma)				
43	95	29,212	0.5	13.2549	3.5	1.8687	3.7	0.1796	1.2	0.32	1065	12	1070	25	1080	71	1065	12	1
25	185	34,089	0.4	12.7710	0.6	2.0058	3.5	0.1858	3.5	0.99	1098	35	1117	24	1155	12	1098	35	5
50	47	29,503	0.3	12.9149	2.0	2.1124	3.2	0.1979	2.5	0.78	1164	26	1153	22	1132	40	1164	26	-3
56	41	17,432	0.8	12.6608	4.5	2.0346	5.5	0.1868	3.2	0.58	1104	33	1127	38	1172	90	1104	33	6
60	44	16,415	0.4	12.6538	3.5	2.1246	3.6	0.1950	1.1	0.30	1148	12	1157	25	1173	68	1148	12	2
67	150	110,758	0.6	12.4647	1.1	2.2265	1.6	0.2013	1.2	0.73	1182	13	1189	11	1203	22	1182	13	2
95	547	47,997	0.2	12.2536	0.4	2.2386	1.3	0.1989	1.2	0.94	1170	13	1193	9	1236	9	1236	9	5
99	376	141,903	1.1	12.0762	0.3	2.4208	1.9	0.2120	1.9	0.98	1240	21	1249	14	1265	7	1265	7	2
94	127	79,005	0.4	11.6542	1.5	2.6145	2.1	0.2210	1.5	0.70	1287	17	1305	16	1334	30	1334	30	4
48	714	36,656	0.2	11.4743	0.2	2.6553	2.2	0.2210	2.1	0.99	1287	25	1316	16	1364	5	1364	5	6
97	85	85,829	0.4	11.2981	1.5	2.9177	3.0	0.2391	2.6	0.87	1382	32	1387	22	1394	28	1394	28	1
83	70	57,312	0.8	10.9707	1.9	3.0301	2.2	0.2411	1.1	0.49	1392	14	1415	17	1450	37	1450	37	4
66	86	91,758	0.4	10.9415	1.4	3.0959	1.8	0.2457	1.1	0.61	1416	14	1432	14	1455	27	1455	27	3
14	76	74,092	0.5	10.9070	1.5	3.1993	1.9	0.2531	1.1	0.60	1454	15	1457	15	1461	29	1461	29	0
82	380	265,962	0.5	9.9039	0.2	3.9000	0.9	0.2801	0.9	0.98	1592	13	1614	8	1642	4	1642	4	3
84	92	56,014	0.9	9.8186	0.9	4.1522	1.3	0.2957	1.0	0.75	1670	15	1665	11	1658	16	1658	16	-1
63	52	61,386	0.8	9.5025	1.6	4.3044	2.6	0.2967	2.0	0.79	1675	30	1694	21	1718	29	1718	29	3
17	89	34,758	0.8	9.2027	0.8	4.5068	2.8	0.3008	2.7	0.95	1695	40	1732	23	1777	15	1777	15	5
10	109	62,539	0.4	8.9157	0.7	4.9217	6.1	0.3183	6.1	0.99	1781	94	1806	52	1835	13	1835	13	3
6	51	37,699	0.3	8.8845	1.2	5.1265	1.5	0.3303	0.9	0.57	1840	14	1841	13	1841	23	1841	23	0
49	210	277,713	0.4	8.5939	0.5	5.8000	1.8	0.3478	1.7	0.96	1924	28	1913	15	1901	9	1901	9	-1
100	35	23,862	1.5	7.1890	2.3	7.1620	3.3	0.3734	2.3	0.70	2045	40	2132	29	2216	40	2216	40	8
65	305	166,053	0.4	6.7524	0.9	8.7905	8.0	0.4305	8.0	0.99	2308	155	2317	73	2324	15	2324	15	1
9	130	100,038	0.3	6.2354	0.3	9.5351	2.1	0.4312	2.1	0.99	2311	40	2391	19	2460	4	2460	4	6
85	44	56,340	0.9	5.8187	0.9	11.2702	4.2	0.4756	4.1	0.98	2508	86	2546	39	2576	14	2576	14	3
74	287	453,546	0.4	5.6935	0.3	12.0885	1.3	0.4992	1.3	0.97	2610	28	2611	12	2612	5	2612	5	0
1	115	138,188	1.4	5.4564	0.2	12.6096	0.9	0.4990	0.9	0.97	2610	20	2651	9	2683	4	2683	4	3
31	169	810,402	0.6	5.3764	0.4	13.6833	1.4	0.5336	1.4	0.96	2756	31	2728	14	2707	7	2707	7	-2
71	53	79,228	0.7	5.3454	0.6	13.4778	1.6	0.5225	1.4	0.91	2710	32	2714	15	2717	11	2717	11	0
34	17	31,434	0.7	5.2606	1.6	13.3873	2.2	0.5108	1.5	0.68	2660	33	2707	21	2743	27	2743	27	3

TABLE 3
(continued)

Grain #	U (ppm)	²⁰⁶ Pb/ ²⁰⁴ Pb	Th/U	Isotope ratios				Apparent ages (Ma)				Disc. (%)									
				²⁰⁶ Pb*/ ²⁰⁷ Pb*	²⁰⁶ Pb*/ ²³⁵ U* (%)	²⁰⁶ Pb*/ ²³⁸ U* (%)	²⁰⁶ Pb*/ ²³⁵ U* (%)	error corr.	²⁰⁶ Pb*/ ²³⁸ U* (Ma)	²⁰⁷ Pb*/ ²³⁵ U* (Ma)	²⁰⁶ Pb*/ ²⁰⁷ Pb* (Ma)		Best age (Ma)								
VL10NB04 (n=85/101)																					
20	220	112,898	0.5	5.2290	0.2	12.4503	2.2	0.4722	2.2	1.00	2493	46	2639	21	2753	4	2753	4	2753	4	9
79	44	105,131	1.3	5.1902	0.7	13.4023	2.9	0.5045	2.8	0.97	2633	60	2708	27	2765	12	2765	12	2765	12	5
52	48	42,751	0.8	5.0383	0.5	14.7635	1.5	0.5395	1.4	0.95	2781	32	2800	14	2814	8	2814	8	2814	8	1
46	193	50,542	0.4	5.0370	0.2	13.7573	2.1	0.5026	2.1	0.99	2625	45	2733	20	2814	4	2814	4	2814	4	7
23	117	240,424	1.0	4.4975	0.2	17.8040	2.2	0.5807	2.2	1.00	2952	53	2979	22	2998	3	2998	3	2998	3	2
Rejected Analyses (>10% discordance, >5% reverse discordance, or >10% 2s age uncertainty)																					
73	247	6,120	0.7	15.5792	8.6	0.6261	13.2	0.0707	10.1	0.76	441	43	494	52	748	182					
58	364	7,030	4.1	12.8648	1.2	1.2126	4.9	0.1131	4.7	0.97	691	31	806	27	1140	23					
29	205	271,147	0.3	14.4684	2.3	1.2510	2.6	0.1313	1.1	0.42	795	8	824	14	902	48					
22	5	2,707	-	12.4411	29.4	1.8947	31.1	0.1710	10.0	0.32	1017	94	1079	210	1206	593					
5	15	9,163	0.6	12.6804	10.6	1.8834	12.3	0.1732	6.2	0.51	1030	59	1075	82	1169	210					
91	12	5,295	1.3	15.0070	16.8	1.6332	17.4	0.1778	4.5	0.26	1055	44	983	110	826	352					
98	34	11,512	0.6	13.5366	7.1	1.8269	7.4	0.1794	2.2	0.29	1063	21	1055	49	1038	144					
37	25	14,443	1.1	13.9992	11.8	1.7672	12.4	0.1794	3.9	0.31	1064	38	1033	81	970	242					
87	38	704	0.3	13.1604	7.7	1.9264	9.2	0.1839	5.1	0.55	1088	51	1090	62	1095	155					
78	47	20,528	0.4	12.1887	4.8	2.0986	5.3	0.1855	2.1	0.40	1097	22	1148	36	1247	95					
32	372	69,890	0.3	12.0378	0.8	2.1629	1.5	0.1888	1.3	0.87	1115	13	1169	11	1271	15					
86	17	10,374	0.6	11.1213	4.9	2.6236	7.2	0.2116	5.3	0.73	1237	59	1307	53	1424	95					
26	18	11,363	0.8	12.2729	7.0	2.5099	7.4	0.2234	2.5	0.33	1300	29	1275	54	1233	138					
40	14	14,595	0.7	11.0941	10.9	2.8150	12.7	0.2265	6.5	0.51	1316	78	1360	96	1428	209					
72	76	162,957	0.4	5.5473	0.4	10.3180	2.8	0.4151	2.7	0.99	2238	52	2464	26	2655	7					
VL10NB05 (n=93/100)																					
60	340	71,649	0.4	17.7591	2.1	0.5647	2.5	0.0727	1.3	0.54	453	6	455	9	465	46					
57	666	136,526	0.5	17.7032	0.7	0.5678	1.1	0.0729	0.8	0.79	454	4	457	4	472	14					
43	178	41,423	0.5	17.5422	2.5	0.5733	3.1	0.0729	1.8	0.59	454	8	460	12	492	55					
75	183	34,578	0.4	17.8276	3.9	0.5665	4.0	0.0733	1.0	0.26	456	5	456	15	456	86					
56	749	138,368	0.5	17.6600	0.7	0.5734	0.9	0.0734	0.5	0.59	457	2	460	3	477	16					

TABLE 3
(continued)

Grain #	U (ppm)	²⁰⁶ Pb/ ²⁰⁴ Pb	Th/U	Isotope ratios				Apparent ages (Ma)				Disc. (%)							
				²⁰⁶ Pb*/ ²⁰⁷ Pb*	\pm (%)	$\frac{^{206}\text{Pb}^*}{^{238}\text{U}}$ (%)	error corr.	²⁰⁷ Pb*/ ²³⁵ U	\pm (Ma)	²⁰⁶ Pb*/ ²³⁸ U*	\pm (Ma)		Best age (Ma)	\pm (Ma)					
70	224	103,655	0.5	18.0022	2.1	0.5626	2.5	0.0735	1.2	0.50	9	453	9	434	48	457	5	*	
58	202	63,784	0.5	17.8653	3.4	0.5686	3.8	0.0737	1.6	0.42	7	457	14	451	76	458	7	*	
63	121	28,128	0.5	17.6831	4.1	0.5750	4.3	0.0737	1.3	0.31	6	461	16	474	90	459	6	*	
32	219	57,842	0.4	17.9053	3.0	0.5684	3.3	0.0738	1.4	0.42	6	457	12	446	67	459	6	*	
59	301	57,226	0.3	17.6449	2.8	0.5768	3.0	0.0738	1.0	0.34	5	462	11	479	62	459	5	*	
14	106	20,836	0.7	18.2159	5.3	0.5602	5.5	0.0740	1.6	0.28	460	7	452	20	408	118	460	7	*
8	306	61,451	0.6	17.8446	2.1	0.5721	2.3	0.0740	1.0	0.42	460	4	459	9	454	46	460	4	*
77	316	67,219	0.3	17.7070	1.6	0.5778	1.7	0.0742	0.6	0.38	461	3	463	6	471	35	461	3	
13	170	39,286	0.3	17.7339	3.8	0.5774	4.1	0.0743	1.6	0.38	462	7	463	15	468	84	462	7	
24	192	39,048	0.3	17.9455	3.3	0.5715	3.5	0.0744	1.2	0.35	463	5	459	13	441	73	463	5	
47	243	39,031	0.2	17.8910	2.6	0.5736	2.8	0.0744	1.1	0.38	463	5	460	10	448	58	463	5	
45	403	106,624	1.0	17.7059	0.9	0.5799	1.5	0.0745	1.2	0.79	463	5	464	5	471	20	463	5	
68	237	51,751	0.3	17.5305	1.9	0.5858	2.1	0.0745	0.9	0.42	463	4	468	8	493	41	463	4	
35	715	125,497	0.4	17.5847	1.2	0.5841	1.3	0.0745	0.5	0.37	463	2	467	5	486	26	463	2	
10	515	199,627	0.4	17.6415	1.0	0.5826	2.9	0.0745	2.7	0.94	463	12	466	11	479	22	463	12	
62	214	30,462	0.3	17.8271	3.0	0.5765	3.4	0.0745	1.5	0.45	463	7	462	12	456	67	463	7	
88	300	73,005	0.2	17.6317	2.9	0.5832	3.0	0.0746	0.7	0.24	464	3	467	11	480	65	464	3	
44	461	117,661	0.5	17.6966	0.8	0.5814	1.4	0.0746	1.1	0.79	464	5	465	5	472	19	464	5	
94	117	30,355	0.4	17.6911	7.6	0.5824	7.9	0.0747	2.3	0.29	465	10	466	30	473	168	465	10	
48	111	32,418	0.3	18.1962	3.2	0.5663	3.3	0.0747	1.0	0.29	465	4	456	12	410	72	465	4	
12	204	39,695	0.5	17.5396	2.6	0.5877	3.1	0.0748	1.8	0.57	465	8	469	12	492	57	465	8	
89	146	34,698	0.4	17.8322	2.3	0.5782	2.4	0.0748	0.8	0.31	465	3	463	9	455	51	465	3	
40	501	15,007	0.5	17.4793	1.8	0.5900	2.1	0.0748	1.1	0.50	465	5	471	8	500	41	465	5	
9	221	109,024	0.3	17.4879	3.0	0.5901	3.1	0.0748	0.9	0.28	465	4	471	12	499	66	465	4	
25	256	54,765	0.6	17.7317	1.4	0.5828	2.3	0.0749	1.8	0.78	466	8	466	9	468	32	466	8	
42	1713	477,936	0.4	17.6825	0.3	0.5857	0.8	0.0751	0.7	0.90	467	3	468	3	474	8	467	3	
3	337	163,888	0.5	17.7145	1.7	0.5847	2.2	0.0751	1.4	0.64	467	6	467	8	470	38	467	6	
84	753	308,073	0.8	17.7833	0.8	0.5826	1.1	0.0751	0.7	0.64	467	3	466	4	462	18	467	3	
34	238	46,836	0.3	17.7255	1.6	0.5851	1.8	0.0752	0.8	0.45	468	4	468	7	469	35	468	4	

TABLE 3
(continued)

Grain #	U (ppm)	$\frac{^{206}\text{Pb}}{^{204}\text{Pb}}$	Th/U	Isotope ratios				Apparent ages (Ma)						Disc. (%)				
				$\frac{^{206}\text{Pb}^*}{^{207}\text{Pb}^*}$	\pm (%)	$\frac{^{207}\text{Pb}^*}{^{235}\text{U}^*}$	\pm (%)	$\frac{^{206}\text{Pb}^*}{^{238}\text{U}^*}$	\pm (Ma)	$\frac{^{207}\text{Pb}^*}{^{235}\text{U}^*}$	\pm (Ma)	$\frac{^{206}\text{Pb}^*}{^{207}\text{Pb}^*}$	\pm (Ma)		Best age (Ma)	\pm (Ma)		
50	357	112,016	0.3	17.6809	1.7	0.5866	2.0	0.0752	1.1	0.54	468	5	469	8	474	38	468	5
66	125	26,602	0.4	18.1772	6.3	0.5707	6.4	0.0752	0.8	0.13	468	4	458	24	413	142	468	4
52	250	49,570	0.2	17.5753	2.1	0.5909	2.4	0.0753	1.2	0.51	468	6	471	9	488	46	468	6
4	117	15,693	0.5	17.1846	5.8	0.6051	6.0	0.0754	1.8	0.30	469	8	480	23	537	126	469	8
20	617	132,511	0.6	17.7591	1.7	0.5861	1.8	0.0755	0.6	0.35	469	3	468	7	465	37	469	3
36	202	66,517	0.5	17.8852	3.5	0.5820	3.6	0.0755	0.9	0.24	469	4	466	13	449	77	469	4
33	833	212,323	0.4	17.5609	0.7	0.5928	4.1	0.0755	4.0	0.98	469	18	473	15	489	16	469	18
31	236	55,106	0.3	17.8426	3.7	0.5835	3.8	0.0755	0.9	0.23	469	4	467	14	454	82	469	4
74	884	211,046	0.5	17.6270	0.6	0.5907	1.4	0.0755	1.2	0.89	469	6	471	5	481	13	469	6
82	339	118,310	0.2	17.7152	1.6	0.5880	1.7	0.0755	0.8	0.43	469	3	470	7	470	35	469	3
39	424	83,394	0.4	17.7462	1.9	0.5871	2.0	0.0756	0.8	0.37	470	3	469	8	466	42	470	3
37	250	58,246	0.7	17.7305	2.8	0.5879	3.1	0.0756	1.5	0.47	470	7	470	12	468	61	470	7
49	241	74,094	0.6	17.6554	1.7	0.5906	2.3	0.0756	1.4	0.63	470	6	471	8	478	39	470	6
7	840	213,167	0.5	17.6665	1.1	0.5906	1.3	0.0757	0.8	0.58	470	3	471	5	476	23	470	3
69	152	81,476	0.4	18.1710	4.1	0.5743	4.3	0.0757	1.3	0.31	470	6	461	16	414	91	470	6
86	403	94,801	0.4	17.6083	1.4	0.5927	2.2	0.0757	1.7	0.76	470	8	473	8	483	32	470	8
67	977	200,363	0.6	17.6077	0.7	0.5927	1.2	0.0757	0.9	0.78	470	4	470	5	484	16	470	4
93	378	129,231	0.5	17.7281	1.4	0.5894	1.7	0.0758	0.9	0.51	471	4	470	6	468	32	471	4
80	1411	486,104	1.0	17.6139	0.4	0.5936	0.7	0.0758	0.5	0.77	471	2	473	3	483	10	471	2
79	320	46,052	0.6	17.9014	2.4	0.5850	2.7	0.0760	1.1	0.41	472	5	468	10	447	54	472	5
41	585	116,094	0.3	17.7057	1.2	0.5920	1.4	0.0760	0.6	0.46	472	3	472	5	471	27	472	3
5	193	32,044	0.5	18.0341	2.9	0.5816	3.1	0.0761	0.9	0.30	473	4	465	12	430	66	473	4
85	400	90,316	1.4	17.5291	1.3	0.5984	1.6	0.0761	0.9	0.54	473	4	476	6	493	29	473	4
28	700	218,220	0.2	17.6189	0.7	0.5956	1.5	0.0761	1.3	0.87	473	6	474	6	482	16	473	6
22	460	90,462	0.4	17.7376	1.3	0.5917	1.5	0.0761	0.7	0.48	473	3	472	6	467	29	473	3
83	376	125,416	0.5	17.4875	1.6	0.6006	1.9	0.0762	1.1	0.58	473	5	478	7	499	35	473	5
100	202	41,218	0.5	17.6082	2.5	0.5996	3.4	0.0766	2.4	0.69	476	11	477	13	483	55	476	11
11	1739	92,999	0.5	17.6541	0.6	0.5981	1.4	0.0766	1.2	0.88	476	6	476	5	478	14	476	6
92	192	29,586	0.4	17.7006	2.6	0.5966	2.7	0.0766	0.8	0.29	476	4	475	10	472	58	476	4
81	729	103,355	0.6	17.6389	1.0	0.5988	1.5	0.0766	1.1	0.76	476	5	476	6	480	21	476	5

TABLE 3
(continued)

Grain #	U (ppm)	²⁰⁶ Pb/ ²⁰⁴ Pb	Th/U	Isotope ratios				Apparent ages (Ma)						Disc. (%)				
				²⁰⁶ Pb*/ ²⁰⁷ Pb*	\pm (%)	$\frac{^{206}\text{Pb}^*}{^{238}\text{U}}$ (%)	\pm (%)	$\frac{^{206}\text{Pb}^*}{^{235}\text{U}}$ (Ma)	\pm (Ma)	$\frac{^{207}\text{Pb}^*}{^{235}\text{U}}$ (Ma)	\pm (Ma)	$\frac{^{206}\text{Pb}^*}{^{207}\text{Pb}^*}$ (Ma)	\pm (Ma)		Best age (Ma)	\pm (Ma)		
VL10NB05 (n=93/100)																		
87	381	60,475	0.4	17.7808	1.3	0.5945	2.0	0.0767	1.5	0.76	476	7	474	7	462	28	476	7
51	481	201,934	0.6	17.7391	1.4	0.5962	2.0	0.0767	1.4	0.71	476	7	475	8	467	31	476	7
91	165	34,058	0.5	18.3711	3.7	0.5776	3.9	0.0770	1.2	0.31	478	6	463	14	389	83	478	6
95	274	39,825	0.2	17.5482	2.1	0.6052	2.8	0.0770	1.8	0.64	478	8	481	11	491	47	478	8
21	1279	388,849	0.5	17.7269	0.4	0.5992	1.2	0.0770	1.1	0.93	478	5	477	4	469	10	478	5
17	96	77,699	0.7	18.3523	7.1	0.5789	7.6	0.0770	2.6	0.35	478	12	464	28	391	159	478	12
26	353	109,254	0.2	17.5176	2.0	0.6074	2.5	0.0772	1.5	0.60	479	7	482	10	495	44	479	7
96	638	96,516	0.3	17.6560	1.2	0.6035	1.3	0.0773	0.6	0.46	480	3	479	5	477	26	480	3
98	820	236,603	0.7	17.4680	0.8	0.6104	1.8	0.0773	1.6	0.90	480	8	484	7	501	18	480	8
18	130	24,872	0.5	17.6302	4.1	0.6080	4.3	0.0777	1.4	0.31	483	6	482	17	481	91	483	6
23	575	126,867	0.5	17.6116	0.8	0.6089	1.3	0.0778	1.0	0.80	483	5	483	5	483	17	483	5
71	16	2,830	0.4	18.8640	36.3	0.6168	36.6	0.0844	4.3	0.12	522	22	488	143	329	849	522	22
72	62	27,096	0.5	17.6445	10.6	0.6841	10.8	0.0875	1.9	0.18	541	10	529	45	479	236	541	10
61	36	7,375	0.5	16.9372	10.9	0.7230	11.5	0.0888	3.5	0.31	549	18	552	49	569	238	549	18
99	209	81,162	0.7	16.5843	1.7	0.8640	2.7	0.1039	2.1	0.78	637	13	632	13	614	36	637	13
64	73	37,022	0.4	12.7637	2.0	2.0445	2.3	0.1893	1.3	0.54	1117	13	1130	16	1156	39	1117	13
38	290	161,318	0.2	12.3454	0.6	2.2968	0.8	0.2056	0.5	0.61	1206	5	1211	6	1221	12	1221	12
29	259	205,198	0.7	11.6963	0.7	2.6857	1.0	0.2278	0.7	0.68	1323	8	1325	7	1327	14	1327	14
1	175	108,526	0.5	11.6219	0.8	2.6900	1.0	0.2267	0.6	0.60	1317	7	1326	7	1339	15	1339	15
65	99	64,992	0.7	10.5435	1.0	3.5424	1.5	0.2709	1.1	0.74	1545	15	1537	12	1525	19	1525	19
97	175	172,145	0.2	9.7496	0.6	4.2717	1.3	0.3021	1.2	0.90	1701	18	1688	11	1671	11	1671	11
90	251	33,127	0.5	9.6112	0.6	4.0943	2.3	0.2854	2.2	0.97	1619	32	1653	19	1697	10	1697	10
19	385	163,296	0.2	9.5839	0.2	4.2630	1.7	0.3090	1.7	0.99	1673	25	1686	14	1703	4	1703	4
27	248	154,717	0.5	9.4994	0.4	4.4853	1.7	0.2963	1.6	0.97	1736	24	1728	14	1719	8	1719	8
78	213	182,612	0.9	9.4085	0.3	4.5258	2.1	0.3088	2.1	0.99	1735	31	1736	17	1737	6	1737	6
2	370	262,089	0.6	9.3049	0.2	4.4675	1.1	0.3015	1.1	0.98	1699	16	1725	9	1757	4	1757	4
73	48	32,902	1.2	8.1909	1.2	6.0144	1.9	0.3573	1.5	0.79	1969	25	1978	16	1987	21	1987	21
54	101	107,700	0.7	6.5595	1.1	9.4889	1.6	0.4514	1.2	0.74	2402	24	2386	15	2374	18	2374	18
6	48	41,569	0.4	13.4843	3.3	1.8664	3.7	0.1825	1.6	0.43	1081	16	1069	24	1046	67	1046	67

TABLE 3
(continued)

Grain #	U (ppm)	$\frac{^{206}\text{Pb}}{^{204}\text{Pb}}$	Th/U	Isotope ratios				Apparent ages (Ma)						Disc. (%)					
				$\frac{^{206}\text{Pb}^*}{^{207}\text{Pb}^*}$	$\frac{^{206}\text{Pb}^*}{^{235}\text{U}^*}$ (%)	\pm	$\frac{^{207}\text{Pb}^*}{^{235}\text{U}^*}$ (%)	\pm	$\frac{^{206}\text{Pb}^*}{^{238}\text{U}^*}$ (%)	error corr.	\pm	$\frac{^{207}\text{Pb}^*}{^{235}\text{U}^*}$ (Ma)	\pm		$\frac{^{206}\text{Pb}^*}{^{238}\text{U}^*}$ (Ma)	Best age (Ma)	\pm		
VLI0NB05 (n=93/100)																			
46	16	3.463	0.4	17.7894	28.8	0.6547	32.3	0.0845	14.6	0.45	523	73	511.3	130.4	461	651			
30	7	1.624	0.4	19.3481	114.5	0.6062	115.9	0.0851	17.8	0.15	526	90	481.2	476.1	271	946			
76	6	2.946	0.8	2.3979	796.3	4.8960	796.4	0.0851	11.6	0.01	527	59	1801.6	-	3972	13			
16	8	2.726	0.7	-2.6962	1072	-4.5153	1072	0.0883	14.7	0.01	545	77	-	-	-	-			
15	7	1.288	0.4	30.6865	66.2	0.4085	67.4	0.0909	12.8	0.19	561	69	347.8	201.1	-	2139			
53	32	29.862	0.7	13.7518	3.7	1.7948	4.5	0.1790	2.6	0.57	1062	25	1043.6	29.6	1006	76			
55	13	8.058	0.4	13.9691	13.6	1.8569	13.8	0.1881	2.6	0.19	1111	26	1065.9	91.3	974	278			
VLI3NB02 (n=56/66)																			
48	903	14.594	0.4	17.9998	0.6	0.4975	2.6	0.0649	2.5	0.97	406	10	410	9	435	13	406	10	
17	320	7.403	0.4	17.8624	1.0	0.5471	1.9	0.0709	1.6	0.85	441	7	443	7	452	22	441	7	*
65	293	5.989	0.6	17.8879	0.6	0.5613	1.5	0.0728	1.3	0.90	453	6	452	5	449	14	453	6	*
26	826	22.757	0.6	17.6679	0.6	0.5771	2.4	0.0739	2.3	0.97	460	10	463	9	476	13	460	10	
61	761	11.412	1.4	17.4318	0.8	0.5971	1.7	0.0755	1.5	0.88	469	7	475	6	506	18	469	7	
60	171	3.673	0.9	17.7233	1.9	0.5884	4.7	0.0756	4.3	0.92	470	19	470	18	469	41	470	19	
34	332	7.327	0.8	17.5848	0.6	0.5967	2.7	0.0761	2.6	0.97	473	12	475	10	486	14	473	12	
32	221	4.621	0.7	17.6419	1.1	0.6010	1.7	0.0769	1.2	0.75	478	6	478	6	479	24	478	6	
50	204	4.206	2.3	17.4991	2.3	0.6155	2.7	0.0781	1.3	0.48	485	6	487	10	497	52	485	6	
6	353	6.209	0.3	17.2749	2.1	0.6246	3.9	0.0783	3.3	0.84	486	15	493	15	525	47	486	15	
55	186	4.565	0.5	17.7405	1.2	0.6163	1.5	0.0793	0.8	0.57	492	4	487	6	467	26	492	4	
51	179	4.300	1.0	17.4820	1.4	0.6369	2.1	0.0808	1.6	0.75	501	8	500	8	499	30	501	8	
30	636	16.629	0.4	17.3459	0.5	0.6614	1.9	0.0832	1.8	0.96	515	9	515	7	516	11	515	9	
23	90	2.346	1.6	17.5463	1.5	0.6830	2.4	0.0869	1.9	0.77	537	10	529	10	491	34	537	10	
53	75	3.375	0.4	14.0595	0.8	1.5351	1.4	0.1565	1.1	0.81	938	10	945	9	961	17	938	10	2
58	157	6.351	2.2	13.9407	0.6	1.5715	1.7	0.1589	1.6	0.94	951	14	959	10	978	12	951	14	3
7	39	2.086	0.7	13.9203	1.5	1.6129	2.5	0.1628	2.0	0.80	973	18	975	16	981	31	973	18	1
66	144	5.504	0.6	13.8874	3.3	1.6370	5.1	0.1649	3.8	0.76	984	35	985	32	986	67	984	35	0
27	54	2.779	0.3	13.8350	1.3	1.6567	2.0	0.1662	1.5	0.75	991	14	992	12	994	27	991	14	0
59	140	6.298	0.7	13.8332	0.9	1.6666	2.3	0.1672	2.1	0.92	997	19	996	14	994	18	997	19	0

Rejected Analyses (>10% discordance, >5% reverse discordance, or >10% 2s age uncertainty)

TABLE 3
(continued)

Grain #	U (ppm)	$\frac{^{206}\text{Pb}}{^{204}\text{Pb}}$	Th/U	Isotope ratios				Apparent ages (Ma)				Disc. (%)							
				$\frac{^{206}\text{Pb}^*}{^{207}\text{Pb}^*}$	\pm (%)	$\frac{^{207}\text{Pb}^*}{^{235}\text{U}^*}$	\pm (%)	$\frac{^{206}\text{Pb}^*}{^{238}\text{U}^*}$	error corr.	$\frac{^{207}\text{Pb}^*}{^{235}\text{U}}$	\pm (Ma)		$\frac{^{206}\text{Pb}^*}{^{238}\text{U}}$	\pm (Ma)	Best age \pm (Ma)				
VLL3NB02 (n=56/66)																			
4	316	15,973	0.6	13.5905	0.6	1.6501	1.4	0.1627	1.2	0.89	971	11	990	9	1030	13	1030	13	6
2	96	4,528	1.1	13.5720	2.0	1.6885	2.8	0.1662	2.0	0.71	991	18	1004	18	1033	40	991	18	4
63	417	18,489	0.02	13.5556	1.3	1.6238	9.2	0.1596	9.1	0.99	955	80	979	58	1035	26	1035	26	8
12	70	4,025	0.4	13.5477	0.8	1.7983	1.9	0.1767	1.8	0.91	1049	17	1045	13	1036	16	1049	17	-1
3	118	5,914	0.5	13.5475	0.9	1.7090	1.6	0.1679	1.3	0.83	1001	12	1012	10	1036	18	1001	12	3
54	285	13,133	0.4	13.5465	0.6	1.7975	2.3	0.1766	2.2	0.96	1048	22	1045	15	1037	12	1048	22	-1
15	119	6,535	0.5	13.4726	1.0	1.8284	1.4	0.1787	1.0	0.72	1060	10	1056	9	1048	19	1060	10	-1
52	404	21,361	0.2	13.3500	0.8	1.8476	3.0	0.1789	2.9	0.96	1061	28	1063	20	1066	17	1061	28	0
20	140	7,242	0.6	13.3248	1.0	1.9003	1.8	0.1836	1.5	0.83	1087	15	1081	12	1070	20	1087	15	-2
35	133	6,819	0.8	13.2949	0.5	1.8501	1.5	0.1784	1.3	0.93	1058	13	1063	10	1074	11	1058	13	1
22	169	9,139	0.2	13.2699	0.7	1.8311	2.2	0.1762	2.1	0.95	1046	20	1057	14	1078	13	1046	20	3
14	142	8,616	0.4	13.2648	0.7	1.8530	1.1	0.1783	0.8	0.74	1058	8	1065	7	1079	15	1058	8	2
19	250	12,941	0.3	13.2465	0.6	1.8557	1.9	0.1783	1.8	0.95	1058	18	1065	13	1082	12	1058	18	2
16	610	31,408	0.3	13.1896	1.0	1.8569	2.6	0.1776	2.4	0.92	1054	24	1066	17	1090	20	1054	24	3
31	17	995	0.4	13.0583	2.2	1.9887	2.7	0.1883	1.5	0.55	1112	15	1112	18	1110	44	1112	15	0
9	100	5,987	0.7	12.8548	0.7	2.1077	2.2	0.1965	2.1	0.95	1157	22	1151	15	1142	13	1157	22	-1
43	217	11,225	0.6	12.7806	0.6	2.1863	3.1	0.2027	3.1	0.98	1190	33	1177	22	1153	12	1190	33	-3
18	144	9,885	0.5	12.7108	0.5	2.1054	2.2	0.1941	2.1	0.97	1143	22	1151	15	1164	10	1143	22	2
13	100	4,795	1.5	12.7105	3.7	1.9212	4.7	0.1771	2.9	0.61	1051	28	1088	31	1164	74	1164	74	10
28	297	22,502	0.3	11.6632	0.8	2.7270	3.9	0.2307	3.8	0.98	1338	46	1336	29	1332	15	1332	15	0
49	140	10,065	0.5	11.5768	0.6	2.8035	2.9	0.2354	2.8	0.98	1363	35	1356	22	1347	11	1347	11	-1
57	489	34,613	0.4	11.1571	1.1	3.1282	5.8	0.2531	5.7	0.98	1455	75	1440	45	1418	20	1418	20	-3
24	97	7,798	0.5	11.1389	0.7	2.7914	3.2	0.2255	3.1	0.98	1311	37	1353	24	1421	13	1421	13	8
5	512	45,039	0.3	10.8667	1.1	3.2971	4.7	0.2599	4.5	0.97	1489	60	1480	36	1468	21	1468	21	-1
29	516	41,588	0.3	10.8420	1.0	3.2112	3.5	0.2525	3.4	0.96	1451	44	1460	27	1472	19	1472	19	1
11	311	26,442	1.6	10.1779	1.5	3.6103	2.3	0.2665	1.7	0.75	1523	23	1552	18	1591	28	1591	28	4
47	204	16,369	1.2	9.8540	0.7	3.9919	2.2	0.2853	2.0	0.94	1618	29	1633	18	1651	13	1651	13	2
64	409	28,674	0.5	9.5923	1.0	4.3841	2.4	0.3050	2.2	0.91	1716	33	1709	20	1701	18	1701	18	-1
25	307	29,058	0.7	9.2576	1.0	4.7825	6.1	0.3211	6.0	0.99	1795	94	1782	51	1766	17	1766	17	-2
36	255	23,198	0.9	8.8824	0.6	5.2370	1.5	0.3374	1.4	0.93	1874	22	1859	13	1841	10	1841	10	-2

TABLE 3
(continued)

Grain #	U (ppm)	²⁰⁶ Pb/ ²⁰⁴ Pb	Th/U	Isotope ratios				Apparent ages (Ma)						Disc. (%)					
				²⁰⁶ Pb*/ ²⁰⁷ Pb*	²⁰⁶ Pb*/ ²³⁵ U*	± (%)	± (%)	²⁰⁶ Pb*/ ²³⁸ U*	± (%)	²⁰⁷ Pb*/ ²³⁵ U	± (Ma)	²⁰⁶ Pb*/ ²⁰⁷ Pb*	± (Ma)		Best age (Ma)	± (Ma)			
VL13NB02 (n=56/66)																			
38	229	32,322	0.7	5.7600	6.6	11.6735	7.7	0.4877	3.8	0.50	2561	81	2579	72	2593	111	2593	111	1
44	179	25,376	0.9	5.6394	0.7	11.9608	1.5	0.4892	1.3	0.88	2567	28	2601	14	2628	12	2628	12	2
1	226	38,023	0.7	5.4730	0.7	13.0511	2.2	0.5181	2.1	0.94	2691	45	2683	21	2678	12	2678	12	0
62	97	14,685	0.9	5.4461	0.7	13.0989	4.5	0.5174	4.5	0.99	2688	98	2687	43	2686	12	2686	12	0
10	88	14,990	0.7	5.3311	0.7	13.6717	1.5	0.5286	1.3	0.89	2736	29	2727	14	2721	11	2721	11	-1
46	41	6,086	0.8	5.2832	0.9	13.6220	2.0	0.5220	1.8	0.90	2707	40	2724	19	2736	14	2736	14	1
Rejected Analyses (>10% discordance, >5% reverse discordance, or >10% <i>Is</i> age uncertainty)																			
56	2745	7	0.1	1.3162	129.0	-	-	-	-	0.91	-	-	-	-	-	-	-	-	-
33	224	4,092	0.7	17.6117	1.4	0.5350	2.4	0.0683	1.9	0.80	426	8	435	8	483	32	483	32	
40	57	1,189	1.4	18.5846	1.8	0.5285	2.0	0.0712	1.0	0.48	444	4	431	7	363	40	363	40	
42	575	34,361	0.5	12.9697	0.8	2.1370	4.2	0.2010	4.1	0.98	1181	44	1161	29	1124	17	1124	17	
41	331	17,703	0.4	12.5039	0.6	2.4007	1.3	0.2177	1.2	0.90	1270	14	1243	10	1196	11	1196	11	
8	569	20,276	0.4	11.6889	11.6	2.3401	11.7	0.1984	1.6	0.13	1167	17	1225	83	1328	225	1328	225	
37	122	9,860	0.6	10.9291	0.6	3.3845	2.6	0.2683	2.5	0.97	1532	34	1501	20	1457	11	1457	11	
45	320	23,755	0.3	10.7974	0.8	3.5093	3.6	0.2748	3.5	0.97	1565	48	1529	28	1480	16	1480	16	
39	267	16,385	0.6	8.7172	0.9	4.6791	2.3	0.2958	2.1	0.92	1671	31	1764	19	1875	16	1875	16	
21	129	14,604	0.3	6.0552	1.0	9.3378	3.0	0.4101	2.8	0.95	2215	53	2372	28	2509	16	2509	16	
VL10NB06 (n=35/55)																			
26	189	24,022	0.4	17.2655	2.8	0.6775	3.7	0.0848	2.4	0.65	525	12	525	15	527	61	525	12	*
23	207	28,932	0.5	16.8441	3.2	0.7063	3.3	0.0863	0.9	0.27	534	5	543	14	581	69	534	5	*
39	196	34,475	0.3	16.9333	4.3	0.7631	6.4	0.0937	4.7	0.74	578	26	576	28	569	93	578	26	
29	190	47,106	1.5	17.0676	4.9	0.7878	5.0	0.0975	1.2	0.24	600	7	590	22	552	106	600	7	
2	117	48,192	0.8	16.6748	5.5	0.8231	6.6	0.0995	3.7	0.56	612	21	610	30	602	118	612	21	-2
19	91	30,211	1.7	16.2935	7.5	0.8432	7.6	0.0996	1.3	0.18	612	8	621	35	652	160	612	8	6
7	138	13,947	0.4	16.5768	3.4	0.8320	3.7	0.1000	1.3	0.34	615	7	615	17	615	74	615	7	0
34	158	24,204	0.4	16.2881	1.6	0.8483	4.7	0.1002	4.4	0.94	616	26	624	22	653	35	616	26	6
25	140	52,431	0.5	16.4228	4.6	0.8459	4.7	0.1007	1.2	0.26	619	7	622	22	635	98	619	7	3

TABLE 3
(continued)

Grain #	U (ppm)	²⁰⁶ Pb/ ²⁰⁴ Pb	Th/U	Isotope ratios				Apparent ages (Ma)				Disc. (%)								
				²⁰⁶ Pb*/ ²⁰⁷ Pb*	$\frac{^{207}\text{Pb}^*}{^{235}\text{U}^*}$ (%)	$\frac{^{206}\text{Pb}^*}{^{238}\text{U}^*}$ (%)	$\frac{^{206}\text{Pb}^*}{^{238}\text{U}^*}$ (%)	$\frac{^{207}\text{Pb}^*}{^{235}\text{U}^*}$ (Ma)	$\frac{^{206}\text{Pb}^*}{^{238}\text{U}^*}$ (Ma)	$\frac{^{206}\text{Pb}^*}{^{238}\text{U}^*}$ (Ma)	$\frac{^{207}\text{Pb}^*}{^{235}\text{U}^*}$ (Ma)									
VL10NB06 (n=35/55)																				
9	658	47,678	1.5	16.3811	0.9	0.8484	1.2	0.1008	0.8	0.69	619	5	624	6	641	19	619	5	3	
3	140	26,860	1.4	16.5740	3.5	0.8391	3.8	0.1009	1.5	0.38	619	9	619	18	616	76	619	9	-1	
49	229	36,334	0.1	16.5230	2.7	0.8619	3.0	0.1033	1.4	0.48	634	9	631	14	622	57	634	9	-2	
42	127	52,075	1.8	16.2816	4.1	0.8755	4.2	0.1034	1.0	0.23	634	6	639	20	654	89	634	6	3	
15	210	83,028	0.9	16.4398	3.3	0.8684	3.6	0.1035	1.5	0.42	635	9	635	17	633	71	635	9	0	
21	1018	270,328	0.0	16.3784	0.7	0.8720	1.1	0.1036	0.8	0.77	635	5	637	5	641	15	635	5	1	
12	241	80,744	0.5	16.3607	2.4	0.8859	2.6	0.1051	1.1	0.44	644	7	644	12	644	51	644	7	0	
45	291	97,756	0.5	16.0467	0.6	0.9291	1.2	0.1081	1.1	0.88	662	7	667	6	685	12	662	7	3	
10	530	206,413	0.0	16.0012	1.2	0.9319	2.6	0.1081	2.3	0.89	662	15	669	13	691	26	662	15	4	
47	430	60,267	0.4	16.1938	0.7	0.9277	2.3	0.1090	2.1	0.95	667	14	666	11	666	15	667	14	0	
14	630	134,621	0.3	15.8689	1.1	1.0098	1.2	0.1162	0.5	0.42	709	3	709	6	709	22	709	3	0	
37	1116	232,601	0.1	15.7503	1.3	1.0195	3.0	0.1165	2.7	0.91	710	18	714	15	725	27	710	18	2	
4	362	101,462	0.5	15.2178	1.4	1.1573	1.8	0.1277	1.1	0.62	775	8	781	10	797	29	775	8	3	
51	196	57,195	0.7	15.2390	2.9	1.1658	3.9	0.1288	2.6	0.67	781	19	785	21	794	60	781	19	2	
18	199	79,753	0.4	13.9261	0.9	1.6407	1.4	0.1657	1.1	0.78	988	10	986	9	980	18	988	10	-1	
46	110	58,704	0.6	12.1678	1.9	2.4118	2.9	0.2128	2.2	0.75	1244	25	1246	21	1250	38	1250	38	0	
22	116	42,532	0.5	11.3744	2.4	2.7698	9.2	0.2285	8.9	0.97	1327	106	1347	69	1381	46	1381	46	4	
8	145	66,089	0.3	10.7405	1.0	3.1625	1.7	0.2464	1.4	0.81	1420	18	1448	13	1490	19	1490	19	5	
13	157	217,565	0.3	10.4601	0.8	3.5604	1.3	0.2701	1.1	0.80	1541	14	1541	10	1540	15	1540	15	0	
5	404	144,888	0.5	10.4116	0.4	3.6171	1.3	0.2731	1.2	0.95	1557	17	1553	10	1549	8	1549	8	-1	
27	140	83,025	0.6	9.1080	0.8	4.8107	1.7	0.3178	1.4	0.87	1779	22	1787	14	1796	15	1796	15	1	
40	173	108,769	0.8	7.9036	0.6	6.5167	2.2	0.3735	2.1	0.96	2046	37	2048	20	2050	11	2050	11	0	
20	128	155,726	0.5	7.8523	1.1	6.4963	16.4	0.3700	16.4	1.00	2029	285	2045	145	2062	19	2062	19	2	
28	139	100,906	0.7	7.8359	0.7	6.3348	4.4	0.3600	4.3	0.99	1982	73	2023	38	2065	13	2065	13	4	
16	108	169,171	0.9	7.4156	0.8	7.5051	2.1	0.4036	2.0	0.92	2186	36	2174	19	2162	14	2162	14	-1	
<i>Rejected Analyses (>10% discordance, >5% reverse discordance, or >10% 2s age uncertainty)</i>																				
24	220	67,611	0.5	15.7009	11.1	0.5287	57.0	0.0602	55.9	0.98	377	205	431	203	731	235				
44	383	265	0.8	12.9072	21.1	1.0544	21.4	0.0987	3.7	0.17	607	21	731	112	1133	424				

TABLE 3
(continued)

Grain #	U (ppm)	²⁰⁶ Pb/ ²⁰⁶ Pb	Th/U	²⁰⁶ Pb*/ ²⁰⁶ Pb*	Isotope ratios				Apparent ages (Ma)				Disc. (%)					
					±	²⁰⁷ Pb*/ ²³⁵ U*	(%)	±	error corr.	²⁰⁶ Pb*/ ²³⁸ U*	(Ma)	±		²⁰⁷ Pb*/ ²³⁵ U	(Ma)	±	²⁰⁶ Pb*/ ²⁰⁶ Pb*	(Ma)
VL10N/B06 (n=35/25)																		
<i>Rejected Analyses (>10% discordance, >5% reverse discordance, or >10% 2s age uncertainty)</i>																		
35	81	13,397	0.8	15.6985	11.8	0.9077	25.2	0.1034	22.2	0.88	634	134	656	122	732	251		
41	64	14,110	0.5	16.3483	10.6	0.8824	12.6	0.1046	6.9	0.54	641	42	642	60	645	228		
55	561	24,119	0.4	15.5647	1.8	0.9338	3.1	0.1054	2.5	0.81	646	15	670	15	750	38		
11	121	19,101	0.4	15.5781	6.3	0.9354	6.5	0.1057	1.5	0.23	648	9	670	32	748	134		
33	253	56,041	1.3	16.4326	1.0	0.9101	2.2	0.1085	2.0	0.89	664	13	657	11	634	22		
54	183	3,384	0.1	15.8013	4.8	0.9572	9.6	0.1097	8.3	0.86	671	53	682	48	718	103		
17	486	93,527	0.5	16.4388	0.7	0.9500	6.0	0.1133	5.9	0.99	692	39	678	30	633	16		
52	113	78,183	0.7	13.1387	43.5	1.2251	49.6	0.1167	23.7	0.48	712	160	812	284	1098	916		
36	212	81,466	0.7	14.5239	26.4	1.1954	37.2	0.1259	26.2	0.70	765	189	798	209	894	555		
48	143	55,503	0.6	15.7380	10.5	1.1138	29.3	0.1271	27.3	0.93	771	199	760	158	726	223		
6	124	21,733	1.0	15.8389	7.8	1.1119	29.4	0.1277	28.3	0.96	775	207	759	158	713	167		
30	87	37,046	0.4	15.1703	2.9	1.2966	5.0	0.1427	4.0	0.81	860	32	844	28	804	61		
53	886	20,363	0.2	12.1172	0.5	1.9420	22.0	0.1707	22.0	1.00	1016	207	1096	149	1258	10		
32	125	7,522	0.5	12.6683	3.2	2.1342	4.9	0.1961	3.7	0.76	1154	39	1160	34	1171	64		
1	42	5,103	0.6	12.4966	9.0	2.3791	33.1	0.2156	31.8	0.96	1259	364	1236	241	1198	179		
38	57	371	0.5	6.9448	23.6	5.9312	24.4	0.2987	6.2	0.26	1685	92	1966	215	2276	412		
50	64	60,656	0.3	6.6652	34.5	6.6330	545	0.3206	544	1.00	1793	-	2064	-	2346	611		
43	51	9,617	2.0	11.5402	27.4	4.4623	101	0.3735	97.0	0.96	2046	1741	1724	1184	1353	538		
31	53	9,270	0.6	13.1440	52.2	12.7467	175	1.2151	167	0.95	5127	-	2661	-	1097	1125		

TABLE 3
(continued)

Notes:

1. Analyses conducted by LA-MC-ICPMS at the Arizona LaserChron Center following methods of Gehrels and others (2008).
2. All uncertainties are reported at the 1-sigma level, and include only measurement errors.
3. Best age is determined from $^{206}\text{Pb}/^{238}\text{U}$ age for analyses with $^{206}\text{Pb}/^{238}\text{U}$ age < 1200 Ma and from $^{206}\text{Pb}/^{207}\text{Pb}$ age for analyses with $^{206}\text{Pb}/^{238}\text{U}$ age > 1200 Ma.
4. Discordance for ages > 600 Ma is calculated as $(100 - (^{206}\text{Pb}/^{207}\text{Pb} \text{ age} - ^{206}\text{Pb}/^{238}\text{U} \text{ age}) / ^{206}\text{Pb}/^{207}\text{Pb} \text{ age})$. Value is not reported for $^{206}\text{Pb}/^{238}\text{U}$ ages < 600 Ma because of large uncertainty in $^{206}\text{Pb}/^{207}\text{Pb}$ age.
5. Analyses > 600 Ma with > 10% discordance or > 5% reverse discordance are not included. Analyses < 500 Ma that are visually discordant on concordia plot are not included.
6. Analyses with > 10% uncertainty (2-sigma) in Best Age are not included.
7. * denotes $^{206}\text{Pb}/^{238}\text{U}$ ages used in calculation of maximum depositional age ($n \geq 2$ and overlap at 1-sigma level).
8. Systematic errors (at 2-sigma level) for $^{206}\text{Pb}/^{238}\text{U}$ and $^{206}\text{Pb}/^{207}\text{Pb}$ are 2.1% & 0.9% VL10NB02, 1.3% & 0.8% for sample VL10NB04, 1.6% & 0.8% for sample VL10NB05, and 1.6% & 0.9% for sample VL13NB02.
9. U concentration and U/Th are calibrated relative to Sri Lanka zircon standard and are accurate to ~20%.
10. Common Pb correction is from measured ^{204}Pb with common Pb composition interpreted from Stacey and Kramers (1975).
11. Common Pb composition assigned uncertainties of 1.5 for $^{207}\text{Pb}/^{204}\text{Pb}$, 0.3 for $^{207}\text{Pb}/^{209}\text{Pb}$, and 2.0 for $^{208}\text{Pb}/^{209}\text{Pb}$.
12. U/Pb and $^{206}\text{Pb}/^{207}\text{Pb}$ fractionation is calibrated relative to fragments of a large Sri Lanka zircon of 563.5 ± 3.2 Ma (2-sigma).
13. U decay constants and composition as follows: $^{238}\text{U} = 9.8485 \times 10^{-10}$, $^{235}\text{U} = 1.55125 \times 10^{-10}$, $^{238}\text{U}/^{235}\text{U} = 137.88$.

(*ca.* 0.9–1.2 Ga) grains. All plots display a large gap from *ca.* 500 to 950 Ma, a series of late Paleoproterozoic to Mesoproterozoic peaks between 1.0 and 1.8 Ga, and a few Neoproterozoic grains in the 2.6 to 3.0 Ga range. In contrast, Neoproterozoic to Cambrian ages (*ca.* 500–1000 Ma) are dominant in zircon grains from the Miramichi Group (VL10-NB06), and the maximum depositional age of the youngest population is 533 ± 8 Ma (fig. 14).

Constraints on Detrital Zircon Provenance

All samples of synaccretionary sedimentary rocks of the Tomogonops, Val Michaud, Elmtree and Duncans Brook formations are dominated by Ordovician zircon populations, but display several peaks in the Mesoproterozoic to late Paleoproterozoic range (*ca.* 1000–1850 Ma) and, except for the Elmtree Formation, small clusters of Neoproterozoic grains between 2.6 and 3.0 Ga (fig. 13). This age profile has many features in common with Laurentia-derived sedimentary rocks. For example, Cawood and Nemchin (2001) assigned detrital zircons from the eastern Laurentian margin in Newfoundland to four major groups: 1. Archean (2600–2850 Ma), affiliated with the Superior craton; 2. Paleoproterozoic (1750–1950 Ma), associated with the Ungava, New Quebec and Torngat orogenic belts; 3. Mesoproterozoic to early Neoproterozoic (950–1450 Ma), related to the Grenvillian orogenic cycle (see also McLelland and others, 1996; Chiarenzelli and others, 2015); and 4. a local Neoproterozoic population (570–760 Ma) associated with rifting that opened the Iapetus ocean. Furthermore, the age spectra of the New Brunswick samples are almost identical to those documented in the Badger Group of Newfoundland (Waldron and others, 2012) and Southern Uplands of Scotland (Waldron and others, 2008), which were similarly ascribed to Laurentian sources. Conversely, a notable feature of the probability density plots for the synaccretionary rocks (fig. 13) is the near complete absence of Neoproterozoic (550–900 Ma) and early Paleoproterozoic (2.0–2.5 Ga) grains. Zircons that sample these intervals are typical of Amazonian (Gondwanan) sources (Teixeira and others, 1989; Barr and others, 2012), and characterize Neoproterozoic to Early Ordovician sedimentary rock units in New Brunswick (Fyffe and others, 2009). Thus, detrital zircon data strongly favor a Laurentian provenance for the Late Ordovician to mid-Silurian units discussed herein.

Detrital zircon probability density plots for all synaccretionary sedimentary rocks demonstrate that the bulk of constituent zircons range in age from *ca.* 440 to 475 Ma (fig. 13). The probable source of this large influx of eroded material was a tectonically uplifted region created by the (late Taconic) collision between the Popelogan arc and the Laurentian margin (van Staal and others, 1998, 2007; Wilson and others, 2004; Zagorevski and others, 2008; Reusch and van Staal, 2012). In Newfoundland, Late Cambrian to Ordovician detrital zircons in the Badger Group were attributed to a source in the Notre Dame arc (Pollock and others, 2007; Waldron and others, 2012). It is likely that zircons in the New Brunswick rocks were also dominantly sourced from the Notre Dame arc because they exhibit Laurentian inheritance, as discussed above, rather than the Ganderian signature that would be expected if the (Ganderian) Popelogan arc were being sampled (compare Dupuis and others, 2009). Furthermore, except for possible small uplifted areas, the Popelogan arc formed the substrate to much of the Matapedia cover. Another potential source is arc magmatic activity associated with Tetagouche backarc subduction; however, that volcanism is younger than the youngest zircon populations in the sampled units.

No detrital zircon data are available for Middle to early Late Ordovician rocks of the Bathurst and Fournier supergroups except for xenocrystic zircons in conglomerate cobbles at the base of the Tetagouche Group (van Staal and others, 1996). However, detrital zircon data from the Knights Brook Formation (Miramichi Group) (sample VL10-NB06; table 3 and fig. 14) show a dominance of grains in the Neoproterozoic

interval that is not represented in the synaccretionary (Late Ordovician and younger) rocks. This profile, showing clear Gondwanan/Ganderian inheritance, is very similar to that obtained from correlative rocks of the Ganderian Woodstock Group (fig. 1) in southwestern New Brunswick (Fyffe and others, 2009). Ganderian provenance is also evident in inherited zircons contained in the 473 ± 4 Ma Meridian Brook Granite (fig. 2) in the southwestern part of the Miramichi Highlands (Roddick and Bevier, 1995). Additionally, the evidence of faunal provincialism in the Bathurst Supergroup, including Sandbian conodonts of North Atlantic affinity (Nowlan, 1981; Nowlan and others, 1997), and Floian – Dapingian brachiopods of the Celtic province (Neuman, 1971, 1984) indicate that the dominant influence during the Early to early Late Ordovician was from the Baltic – Gondwanan realm rather than from Laurentia. It is therefore clear that the Late Ordovician in the northern Appalachians is accompanied by a dramatic transition in sedimentary input from primarily east (present coordinates), to primarily west.

DISCUSSION

Darriwilian – Katian pelagic chert and overlying shale in the upper part of the Bathurst Supergroup are overlain by significantly thicker units of dominantly siliciclastic turbidites that are correlated with turbidites in the Grog Brook and Matapedia groups of the Matapedia forearc basin, and with equivalent rocks of the Badger Group in Newfoundland. This abrupt lithological change signifies sharply contrasting depositional styles and tectonic environments, which we have ascribed to a transition from oceanic conditions far removed from a cratonic source area, to a trench setting (van Staal and others, 2003, 2008). This interpretation is also consistent with the change in sediment provenance indicated by the detrital zircons. Detrital zircon evidence and faunal affinities demonstrate that, before the Late Ordovician, sedimentary rocks of the Bathurst and Fournier supergroups had a Ganderian/Gondwanan provenance. In contrast, the overlying, Upper Ordovician to Wenlockian synaccretionary rocks have a Laurentian provenance, supporting the lithological correlation with the Grog Brook and Matapedia groups, which also have a Laurentian provenance based on fossils (Fyffe and Fricker, 1987; Boucot, 1993; Nowlan and others, 1997) and volcanic detritus (Dupuis and others, 2009). Hence, all were connected to composite Laurentia.

Scarcity of outcrop and fossils, and structural complexities in critical areas of New Brunswick, precludes clear recognition of whether or not the ‘pelagic’ and ‘turbidite’ successions are conformable. The pelagic rocks in the upper part of the Little River, Boucher Brook and Elmtree formations contain graptolites that have mainly been assigned to the *N. gracilis* to *Dicranograptus clingani* zones, ranging in age from late Darriwilian to early Katian (Ami, 1905; Alcock, 1935 and references therein; Skinner, 1974; Langton and McDonald, 1995; McCutcheon and others, 1995). Trilobites and conodonts in local occurrences of limestone (Helmstaedt, 1971; Skinner, 1974; Kennedy and others, 1979; Nowlan, 1981) and radiometric ages (*ca.* 457 Ma) of peralkaline rhyolite in the upper part of the Bathurst Supergroup (Sullivan and van Staal, 1996) also indicate a late Darriwilian to early Katian age range. However, a graptolite assemblage from the Little River Formation at a location near Bathurst has been assigned to the *Climacograptus spiniferus* zone by Riva and Malo (1988); this middle Katian age coincides with the oldest age attributed to the Grog Brook Group in the Matapedia forearc basin (Riva and Malo, 1988). Similar relationships are revealed by equivalent successions elsewhere in the northern Appalachians. In Newfoundland, Sandbian to early Katian black shale of the Lawrence Harbour and correlative formations overlies volcanic rocks of the Victoria arc (equivalent to the Popelogan arc) and is overlain conformably by the Badger Group. Basal units of the Badger Group (for example, the Point Leamington Formation) comprise Katian siliciclastic turbidites (Williams and others, 1995; Waldron and others, 2012) very similar to those of the

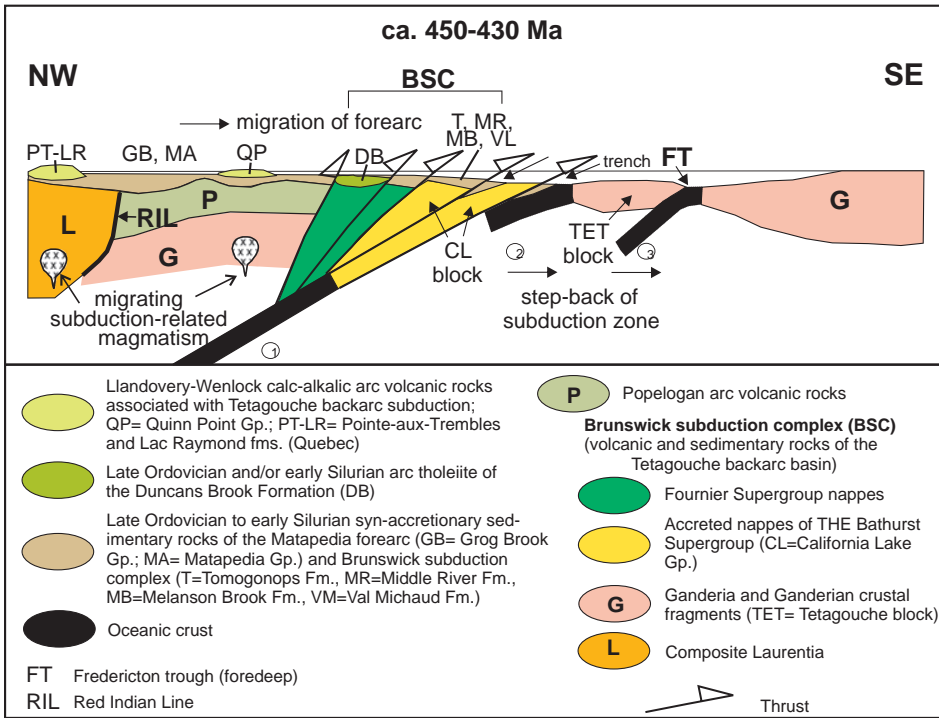


Fig. 15. Schematic tectonic model showing a Late Ordovician stage in the development of the Brunswick subduction complex and associated, Late Ordovician to Wenlockian (ca. 450–430 Ma) migrating arc magmatism. Numbers outline the sequential stepping-back of the subduction zone over time concurrent with progressive onlap of Matapedia cover on accreted material.

Grog Brook Group, and by extension, the Tomogonops and Middle River formations in the Bathurst Supergroup. Graptolite assemblages in the Point Leamington Formation are similar to those in the upper part of the Tetagouche Group, and overlap with the mid to late Katian age of graptolites in Grog Brook-equivalent rocks of the Garin Formation in Quebec, which range from the *C. spiniferus* to *Paraclimacograptus manitoulinensis* zones (Riva and Malo, 1988). A conformable transition from pelagic black shale to mid Katian and younger, synaccretionary sedimentary rocks of the Bathurst and Fournier supergroups is therefore probable, at least locally (fig. 3). Elsewhere, relationships may either be tectonic or disconformable (see above).

The oldest, conformable parts of the Tomogonops, Melanson Brook, Middle River and Val Michaud formations are interpreted to have been deposited as wedge-top and foredeep clastic wedges (DeCelles and Giles, 1996) during accretion of the underlying elements of the Tetagouche backarc basin to the leading edge of composite Laurentia (Matapedia forearc basin). The Laurentian provenance and lithological resemblance of synaccretionary deposits of the Bathurst Supergroup to the Grog Brook and Matapedia groups implies that the former represent a ‘spillover’ of forearc sedimentary material into the trench or onto a progressively deforming subduction complex during, and probably following, exhumation of part of the subduction complex nappes. In other words, the forearc migrated trenchward in lockstep with piecemeal accretion of backarc crustal slivers having Ganderian continental substrates (fig. 15) and consequent, stepwise retreat of the subduction zone (van Staal and others, 2003, 2008; Wilson and others, 2008). A small inlier of dark gray,

Matapedia-like calcilutite located west of the Elmtree inlier (fig. 1) probably represents the remnant of an intermediate depozone between the subduction complex to the east (present coordinates) and the main forearc belt in the Aroostook – Percé Anticlinorium to the west (fig. 1). Once the underlying Tetagouche element was accreted, turbidite sedimentation may have continued, but now as part of an accretionary-wedge slope or an onlapping forearc basin. If so, there may be cryptic unconformities in the turbidite successions, which would be consistent with the apparently conflicting, conformable and unconformable/tectonic field relationships observed between the turbidites and underlying rocks from one locality to another.

Other criteria that potentially can be used to differentiate between syn-accretion (foredeep) and post-accretion depositional settings are differences in metamorphic grade and structural evolution among the various units. However, the heterogeneity of deformation, characterized by marked strain gradients and variations in metamorphic grade ranging locally from prehnite-pumpellyite facies to blueschist and/or high-pressure greenschist facies conditions, compounded by tectonic shuffling as a result of out-of-sequence thrusting and normal faulting (van Staal and others, 2001, 2008), render these criteria generally ambiguous. The problem of pre-accretion foredeep/trench deposition vs. post-accretion piggy-back basins is difficult to resolve, given the generally poor exposure and evidence in hand, but five lines of evidence support the interpretation that some turbidites were deposited on a growing and deforming Brunswick subduction complex: 1. The inferred late Ordovician – early Silurian age of the Tomogonops and Val Michaud formations (and indirectly the Middle River and Melanson Brook formations) based on detrital zircons coincides with the formation of D_1/M_1 blueschist and high-pressure greenschist facies rocks based on $^{40}\text{Ar}/^{39}\text{Ar}$ ages of phengite (van Staal and others, 2003); 2. deformation is time-transgressive (van Staal and others, 2003, 2008), and elements of the Tetagouche Group were accreted after those of the Fournier Supergroup and California Lake Group; thus, the Laurentia-derived sediments that formed the basal part of the Tomogonops Formation had to move across the earlier accreted nappes; 3. evidence of tectonic contacts along the western or northwestern margins of the Middle River and Val Michaud formations (fig. 2), such as narrow zones of mélange along the contact between the Boucher Brook and Middle River formations (fig. 9), supports active D_1 thrusting as deposition occurred; 4. indications are that some contacts between the turbidites and the underlying rocks are unconformable; and 5. the Duncans Brook arc basalt and underlying sandstone lie unconformably above the Devereaux Complex (fig. 4) of the Fournier Supergroup, which occupies the structurally highest nappe in the Brunswick subduction complex. The trench-proximal location of these volcanic and sedimentary rocks is best explained by southeast-directed migration of the Salinic arc towards its trench, such that the arc basalt now erupted into what was previously part of the arc-trench gap. The foregoing suggests that turbidites in the Brunswick subduction complex that resemble those of the Matapedia forearc basin were probably originally deposited in syn-accretion clastic basins in the wedge-top and proximal foredeep, but over time became part of a trench-migrating accretionary forearc basin as the Tetagouche backarc subduction zone stepped to the southeast behind accreted blocks (compare Dickinson and Seely, 1979; fig. 15). The end of Tetagouche backarc basin subduction at *ca.* 430 Ma coincided with collision of the Gander margin and composite Laurentia, leading to uplift associated with Salinic orogenesis and inversion of the Matapedia forearc basin.

CONCLUSIONS

Upper Ordovician to Llandoveryan synaccretionary, mainly turbiditic sedimentary rocks of the Bathurst and Fournier supergroups were deposited, at least in part, conformably above Sandbian – Katian pelagic sediments (chert and black shale) during incorporation of their substrate of backarc basin rocks into the Brunswick

subduction complex. Accretion started shortly after the initiation of northwest-directed Salinic subduction of the Tetagouche backarc basin at *ca.* 450 Ma, because the backarc basin contained several buoyant blocks of extended continental backarc crust, as well as basaltic seamounts that resisted deep subduction (van Staal and others, 2008). Detrital zircon analysis indicates that the youngest zircon populations in the Tomogonops and Val Michaud formations are Sandbian to Katian, implying that deposition of these units was coeval with deposition of lithologically similar, Late Ordovician to Silurian rocks in the Matapedia cover sequence.

The age of the Duncans Brook Formation is latest Ordovician to early Silurian, based on detrital zircon populations in underlying and interlayered sedimentary rocks, confirming the hypothesis of Winchester and others (1992) that these rocks are significantly younger than other basalt in the Elmtree inlier. Hence, the Duncans Brook Formation is interpreted to unconformably overlie the Middle Ordovician rocks of the Devereaux Complex. The Duncans Brook basalt has arc tholeiitic compositions and is probably tectonically related to somewhat younger (late Llandoveryan) calc-alkaline basalt in the Weir Formation (Quinn Point Group) farther to the northwest (Wilson and others, 2008).

All age constraints show that deposition of the Matapedia cover sequence took place while northwest-directed subduction and deformation within the Brunswick subduction complex was occurring farther east in the adjacent Tetagouche backarc basin; that is, the depositional setting of the Matapedia cover sequence was a forearc basin. The implication of this 'spillover' of forearc rocks into and onto the adjacent trench and accretionary wedge is that the forearc progressively expanded toward the southeast between *ca.* 450 and 430 Ma; this is attributed to Late Ordovician – Llandoveryan (Salinic) accretion of buoyant blocks in the Tetagouche backarc basin to composite Laurentia, and concomitant stepping back of the subduction zone. The foregoing demonstrates the complex interplay between accretion, sedimentation and exhumation in a large accretionary forearc system. Accretion ended with the arrival of the leading edge of the Gander margin no later than 430 Ma, marking the culmination of Salinic orogenesis.

ACKNOWLEDGMENTS

Critical review by L.R. Fyffe of an early draft of the manuscript is gratefully acknowledged. The paper has greatly benefited from careful reviews by John Waldron and Alex Zagorevski, and the comments of journal Associate Editor Robert Wintsch. Part of this research was carried out under the auspices of the Targeted Geoscience Initiative (TGI) of the Geological Survey of Canada. Analytical funding was provided in part by U.S. National Science Foundation grants EAR-0948359 and EAR-1049368 to McClelland and EAR 1032156 to the University of Arizona Laserchron Center.

REFERENCES

- Alcock, F. J., 1935, Geology of the Chaleur Bay region: Geological Survey of Canada, Memoir 183, 146 p.
- Ami, H. M., 1905, Appendix to summary report for 1904 by L.W. Bailey: Geological Survey of Canada Summary Report 1904, p. 289–292.
- Ayrton, W. G., Berry, W. B. N., Boucot, A. J., Lajoie, J., Lespérance, P. J., Pavlides, L., and Skidmore, W. B., 1969, Lower Llandovery of the Northern Appalachians and adjacent regions: Geological Society of America Bulletin, v. 80, n. 3, p. 459–484, [http://dx.doi.org/10.1130/0016-7606\(1969\)80\[459:LLOTNA\]2.0.CO;2](http://dx.doi.org/10.1130/0016-7606(1969)80[459:LLOTNA]2.0.CO;2)
- Barr, S. M., Hamilton, M. A., Samson, S. D., Satkoski, A. M., and White, C. E., 2012, Provenance variations in northern Appalachian Avalonia based on detrital zircon patterns in Ediacaran and Cambrian sedimentary rocks, New Brunswick and Nova Scotia, Canada: Canadian Journal of Earth Sciences, v. 49, n. 3, p. 533–546, <http://dx.doi.org/10.1139/e11-070>
- Black, L. P., Kamo, S. L., Allen, C. M., Davis, D. W., Aleinikoff, J. N., Valley, J. W., Mundil, R., Campbell, I. H., Korsch, R. J., Williams, I. S., and Foudoulis, C., 2004, Improved $^{206}\text{Pb}/^{238}\text{U}$ microprobe geochronology by the monitoring of a trace-element-related matrix effect; SHRIMP, ID-TIMS, ELA-ICP-MS and oxygen

- isotope documentation for a series of zircon standards: *Chemical Geology*, v. 205, n. 1–2, p. 115–140, <http://dx.doi.org/10.1016/j.chemgeo.2004.01.003>
- Boucot, A. J., 1993, Comments on Cambrian-to-Carboniferous biogeography and its implications for the Acadian Orogeny, *in* Roy, D. C., and Skehan, J. W., editors, *The Acadian Orogeny: Recent Studies in New England, Maritime Canada, and the Autochthonous Foreland*: Geological Society of America Special Papers, v. 275, p. 41–49, <http://dx.doi.org/10.1130/SPE275-p41>
- Cawood, P. A., and Nemchin, A. A., 2001, Paleogeographic development of the east Laurentian margin: Constraints from U-Pb dating of detrital zircons in the Newfoundland Appalachians: *Geological Society of America Bulletin*, v. 113, n. 9, p. 1234–1246, [http://dx.doi.org/10.1130/0016-7606\(2001\)113<1234:PDOTEL>2.0.CO;2](http://dx.doi.org/10.1130/0016-7606(2001)113<1234:PDOTEL>2.0.CO;2)
- Chiarenzelli, J., Kratzmann, D., Selleck, B., and deLorraine, W., 2015, Age and provenance of Grenville supergroup rocks, Trans-Adirondack Basin, constrained by detrital zircons: *Geology*, v. 43, n. 2, p. 183–186, <http://dx.doi.org/10.1130/G36372.1>
- David, J., and Gariépy, C., 1990, Early Silurian orogenic andesites from the central Quebec Appalachians: *Canadian Journal of Earth Sciences*, v. 27, n. 5, p. 632–643, <http://dx.doi.org/10.1139/e90-060>
- Dawson, K. R., 1961, *Geology, Sevege, Northumberland and Gloucester counties, New Brunswick*: Geological Survey of Canada, Map 1092A (with descriptive notes).
- DeCelles, P. G., and Giles, K. A., 1996, Foreland basin systems: *Basin Research*, v. 8, n. 2, p. 105–123, <http://dx.doi.org/10.1046/j.1365-2117.1996.01491.x>
- Dickinson, W. R., and Gehrels, G. E., 2009, Use of U-Pb ages of detrital zircons to infer maximum depositional ages of strata: A test against a Colorado Plateau Mesozoic database: *Earth and Planetary Science Letters*, v. 288, n. 1–2, p. 115–125, <http://dx.doi.org/10.1016/j.epsl.2009.09.013>
- Dickinson, W. R., and Seely, D. R., 1979, Structure and stratigraphy of forearc regions: *AAPG Bulletin*, v. 63, n. 1, p. 2–31.
- Dupuis, C., Malo, M., Bédard, J., Davis, B., and Villeneuve, M., 2009, A lost arc – back-arc terrane of the Dunnage oceanic tract recorded in clasts from the Garin Formation and McCrea mélange in the Gaspé Appalachians of Québec: *Geological Society of America Bulletin*, v. 121, n. 1–2, p. 17–38, <http://dx.doi.org/10.1130/B26251.1>
- Fyffe, L. R., 1976, Correlation of geology in the southwestern and northern parts of the Miramichi Zone: 139th Annual Report, New Brunswick Department of Natural Resources, Province of New Brunswick, p. 137–141.
- Fyffe, L. R., and Fricker, A., 1987, Tectonostratigraphic terrane analysis of New Brunswick: Maritime Sediments and Atlantic Geology, v. 23, n. 3, p. 113–122, <http://dx.doi.org/10.4138/1626>
- Fyffe, L. R., McCutcheon, S. R., and Wilson, R. A., 1997, Miramichi – Tetagouche Group stratigraphic relationships, Bathurst Mining Camp, *in* Carroll, B. M. W., editor, *Current Research 1996: New Brunswick* New Brunswick Department of Natural Resources and Energy, Minerals Division, Mineral Resources Report 97-4, p. 37–51.
- Fyffe, L. R., Barr, S. M., Johnson, S. C., McLeod, M. J., McNicoll, V. J., Valverde-Vaquero, P., van Staal, C. R., and White, C. E., 2009, Detrital zircon ages from Neoproterozoic and Early Paleozoic conglomerate and sandstone units of New Brunswick and coastal Maine: Implications for the tectonic evolution of Ganderia: *Atlantic Geology*, v. 45, p. 110–144, <http://dx.doi.org/10.4138/atgeol.2009.006>
- Fyffe, L. R., Johnson, S. C. and van Staal, C. R., 2011, A review of Proterozoic to Early Paleozoic lithotectonic terranes in New Brunswick, Canada, and their tectonic evolution during Penobscot, Taconic, Salinic, and Acadian orogenesis: *Atlantic Geology*, v. 47, p. 211–248, <http://dx.doi.org/10.4138/atgeol.2011.010>
- Gehrels, G. E., Valencia, V., and Pullen, A., 2006, Detrital zircon geochronology by Laser-Ablation Multicollector ICPMS at the Arizona LaserChron Center, *in* Loszewski, T. and Huff, W., editors, *Geochronology: Emerging Opportunities*: Paleontological Society Short Course, Paleontology Society Papers, v. 11, 10 p.
- Gehrels, G. E., Valencia, V. A., and Ruiz, J., 2008, Enhanced precision, accuracy, efficiency, and spatial resolution of U-Pb ages by laser ablation-multicollector-inductively coupled plasma-mass spectrometry: *Geochemistry, Geophysics, Geosystems*, v. 9, n. 3, Q03017, <http://dx.doi.org/10.1029/2007GC001805>
- Helmstaedt, H., 1971, Structural geology of Portage Lakes area, Bathurst–Newcastle District, New Brunswick: Geological Survey of Canada, Paper 70–28, 52 p., <http://dx.doi.org/10.4095/105650>
- Hibbard, J. P., van Staal, C. R., and Rankin, D. W., and Williams, H., 2006, Lithotectonic map of the Appalachian Orogen (North), Canada-United States of America: Geological Survey of Canada, Map 02042A, scale 1:1,500,000.
- Irrinki, R. R., 1971, Forks of Tomogonops, Portage and Northwest Miramichi rivers, map area P–9: New Brunswick Department of Natural Resources and Energy, Minerals and Energy Division, Plate 71–44.
- Kennedy, D. J., Barnes, C. R., and Uyeno, T. T., 1979, A Middle Ordovician conodont faunule from the Tetagouche Group, Camel Back Mountain, New Brunswick: *Canadian Journal of Earth Sciences*, v. 16, n. 3, p. 540–551, <http://dx.doi.org/10.1139/e79-049>
- Langton, J. P., 1993, Tomogonops project, NTS 21 P/4 west, Gloucester County, New Brunswick, *in* Abbott, S. A., compiler, *Abstracts/Résumés for 1993*: New Brunswick Department of Natural Resources and Energy, Minerals and Energy Division, Information Circular 93–3, p. 31–32.
- 1995, *Geology of the Big Sevege River area (NTS 21 P/4c, d), Bathurst Mining Camp, New Brunswick*, *in* Langton, J. P., editor, *Geoscience Research 1994*: New Brunswick Department of Natural Resources and Energy, Minerals and Energy Division, Miscellaneous Report 15, p. 100–107.
- 1996, Relative age, stratigraphic position, and provenance of new sedimentary formations in the eastern Bathurst Camp, New Brunswick, *in* Carroll, B. M. W., editor, *Current Research 1995*: New Brunswick Department of Natural Resources and Energy, Minerals and Energy Division, Mineral Resource Report 96-1, p. 61–71.

- Langton, J. P., and McDonald, S., 1995, Geology of the Big Sevole River area (NTS 21 P/4c, d), Bathurst Mining Camp, New Brunswick, in Merlini, S. A. A., editor, Current Research 1994: New Brunswick Department of Natural Resources and Energy, Minerals and Energy Division, Miscellaneous Report 18, p. 59–80.
- Ludwig, K. R., 2003, User's manual for Isoplot (3.41d): a geochronological toolkit for Microsoft Excel: Berkeley, California, Berkeley Geochronology Center, Special Publication No. 4, 71 p.
- Malo, M., 1988, Stratigraphy of the Aroostook – Percé Anticlinorium in the Gaspé Peninsula, Quebec: Canadian Journal of Earth Sciences, v. 25, n. 6, p. 893–908, <http://dx.doi.org/10.1139/e88-086>
- Malo, M., and Bourque, P.-A., 1993, Timing of the deformation events from Late Ordovician to Mid-Devonian in the Gaspé Peninsula: Geological Society of America Special Papers, v. 275, p. 101–122, <http://dx.doi.org/10.1130/spe275-p101>
- Mattinson, J. M., 2010, Analysis of the relative decay constants of ^{235}U and ^{238}U by multi-step CA-TIMS measurements of closed-system natural zircon samples: Chemical Geology, v. 275, 3–4, p. 186–198, <http://dx.doi.org/10.1016/j.chemgeo.2010.05.007>
- McCutcheon, S. R., Melchin, M. J., and Walker, J. A., 1995, A new Ordovician graptolite locality, Elmtree Formation, northern New Brunswick: Tectonostratigraphic significance, in Merlini, S. A. A., editor, Current Research 1994: New Brunswick Department of Natural Resources and Energy, Minerals and Energy Division, Miscellaneous Report 18, p. 127–140.
- McLelland, J., Daly, J. S., and McLelland, J. M., 1996, The Grenville orogenic cycle (*ca.* 1350–1000 Ma): an Adirondack perspective: Tectonophysics, v. 265, n. 1–2, p. 1–28, [http://dx.doi.org/10.1016/S0040-1951\(96\)00144-8](http://dx.doi.org/10.1016/S0040-1951(96)00144-8)
- Moench, R. H., and Aleinikoff, J. N., 2002, Stratigraphy, geochronology, and accretionary terrane settings of two Bronson Hill arc sequences, northern New England: Physics and Chemistry of the Earth, v. 27, n. 1–3, p. 47–95, [http://dx.doi.org/10.1016/S1474-7065\(01\)00003-1](http://dx.doi.org/10.1016/S1474-7065(01)00003-1)
- Neuman, R. B., 1971, An early Middle Ordovician brachiopod assemblage from Maine, New Brunswick, and northern Newfoundland, in Dutro, J. T., Jr., editor, Paleozoic Perspectives: A Paleontological Tribute to C. Arthur Cooper: Smithsonian Contributions to Paleobiology, No. 3, p. 113–124.
- 1984, Geology and paleobiology of islands in the Ordovician Iapetus Ocean: Review and implications: Geological Society of America Bulletin, v. 95, n. 10, p. 1188–1201, [http://dx.doi.org/10.1130/0016-7606\(1984\)95<1188:GAPOII>2.0.CO;2](http://dx.doi.org/10.1130/0016-7606(1984)95<1188:GAPOII>2.0.CO;2)
- Nowlan, G. S., 1981, Some Ordovician conodont faunules from the Miramichi Anticlinorium, New Brunswick: Geological Survey of Canada, Bulletin 345, 35 p., <http://dx.doi.org/10.4095/119435>
- Nowlan, G. S., McCracken, A. D., and McLeod, M. J., 1997, Tectonic and paleogeographic significance of Late Ordovician conodonts in the Canadian Appalachians: Canadian Journal of Earth Sciences, v. 34, n. 11, p. 1521–1537, <http://dx.doi.org/10.1139/e17-124>
- O'Brien, B. H., 2003, Geology of the Central Notre Dame Bay region (parts of NTS areas 2E/3,6,11), northeastern Newfoundland: Newfoundland and Labrador Department of Mines and Energy, Geological Survey Report 03-03, 147 p.
- Pearce, J. A., 1983, Role of the sub-continental lithosphere in magma genesis at active continental margins, in Hawkesworth, C. J., and Norry, M. J., editors, Continental Basalts and Mantle Xenoliths: Nantwich, Cheshire, Shiva Press, p. 230–249.
- 2008, Geochemical fingerprinting of oceanic basalts with applications to ophiolitic classification and the search for Archean oceanic crust: Lithos, v. 100, n. 1–4, p. 14–48, <http://dx.doi.org/10.1016/j.lithos.2007.06.016>
- Pearce, J. A., and Cann, J. R., 1973, Tectonic setting of basic volcanic rocks determined using trace element analyses: Earth and Planetary Science Letters, v. 19, n. 2, p. 290–300, [http://dx.doi.org/10.1016/0012-821X\(73\)90129-5](http://dx.doi.org/10.1016/0012-821X(73)90129-5)
- Pollock, J. C., Wilton, D. H. C., van Staal, C. R., and Morrissey, K. D., 2007, U-Pb detrital zircon geochronological constraints on the Early Silurian collision of Ganderia and Laurentia along the Dog Bay Line: The terminal Iapetan suture in the Newfoundland Appalachians: American Journal of Science, v. 307, n. 2, p. 399–433, <http://dx.doi.org/10.2475/02.2007.04>
- Rusch, D. N., and van Staal, C. R., 2012, The Dog Bay – Liberty Line and its significance for Silurian tectonics of the northern Appalachian orogeny: Canadian Journal of Earth Sciences, v. 49, p. 239–258, <http://dx.doi.org/10.1139/E11-024>
- Riva, J., and Malo, M., 1988, Age and correlation of the Honorat Group, southern Gaspé Peninsula: Canadian Journal of Earth Sciences, v. 25, n. 10, p. 1618–1628, <http://dx.doi.org/10.1139/e88-154>
- Roddick, J. C., and Bevier, M. L., 1995, U-Pb dating of granites with inherited zircon: Conventional and ion microprobe results from two Paleozoic plutons, Canadian Appalachians: Chemical Geology, v. 119, n. 1–4, p. 307–329, [http://dx.doi.org/10.1016/0009-2541\(94\)00107-j](http://dx.doi.org/10.1016/0009-2541(94)00107-j)
- Rodgers, J., 1970, The Tectonics of the Appalachians: New York, John Wiley and Sons, 271 p.
- St. Peter, C., 1978, Geology of parts of Restigouche, Victoria and Madawaska counties, northwestern New Brunswick, N.T.S. 21 N/8, 21 N/9, 21 O/5, 21 O/11, 21 O/14: New Brunswick Department of Natural Resources, Mineral Resources Branch, Report of Investigations 17, 69 p.
- 1982, Geology of Juniper–Knowlesville–Carlisle area, map areas I–16, I–17, I–18 (parts of 21 J/11 and 21 J/06): New Brunswick Department of Natural Resources, Geological Surveys Branch, Map Report 82-1, 82 p.
- Shervais, J. W., 1982, Ti-V plots and the petrogenesis of modern and ophiolitic lavas: Earth and Planetary Science Letters, v. 59, n. 1, p. 101–118, [http://dx.doi.org/10.1016/0012-821X\(82\)90120-0](http://dx.doi.org/10.1016/0012-821X(82)90120-0)
- Skinner, R., 1974, Geology of Tetagouche Lakes, Bathurst and Nepisiguit Falls map-areas, New Brunswick, with emphasis on the Tetagouche Group: Geological Survey of Canada, Memoir 371, 133 p.
- Stacey, J. S., and Kramers, J. D., 1975, Approximation of terrestrial lead isotope evolution by a two-stage

- model: *Earth and Planetary Science Letters*, v. 26, n. 2, p. 207–221, [http://dx.doi.org/10.1016/0012-821X\(75\)90088-6](http://dx.doi.org/10.1016/0012-821X(75)90088-6)
- Sullivan, R. W., and van Staal, C. R., 1996, Preliminary chronostratigraphy of the Tetagouche and Fournier groups in northern New Brunswick, in *Radiogenic Age and Isotopic Studies*, Report 9: Geological Survey of Canada, Current Research 1995-F, p. 43–56.
- Sun, S.-S., and McDonough, W. F., 1989, Chemical and isotopic systematics of oceanic basalts: Implications for mantle composition and processes: *Geological Society Special Publication No. 42*, p. 313–345.
- Teixeira, W., Tassinari, C. C. G., Cordani, U. G., and Kawashita, K., 1989, A review of the geochronology of the Amazonian Craton: Tectonic implications: *Precambrian Research*, v. 42, n. 3–4, p. 213–227, [http://dx.doi.org/10.1016/0301-9268\(89\)90012-0](http://dx.doi.org/10.1016/0301-9268(89)90012-0)
- Tucker, R. D., and Robinson, P., 1990, Age and setting of the Bronson Hill magmatic arc: A re-evaluation based on U-Pb zircon ages in southern New England: *Geological Society of America Bulletin*, v. 102, n. 10, p. 1404–1419, [http://dx.doi.org/10.1130/0016-7606\(1990\)102<1404:AASOTB>2.3.CO;2](http://dx.doi.org/10.1130/0016-7606(1990)102<1404:AASOTB>2.3.CO;2)
- van Staal, C. R., 1987, Tectonic setting of the Tetagouche Group in northern New Brunswick: Implications for plate tectonic models of the northern Appalachians: *Canadian Journal of Earth Sciences*, v. 24, n. 7, p. 1329–1351, <http://dx.doi.org/10.1139/e87-128>
- 1994, Brunswick subduction complex in the Canadian Appalachians: Record of the Late Ordovician to Late Silurian collision between Laurentia and the Gander margin of Avalon: *Tectonics*, v. 13, n. 4, p. 946–962, <http://dx.doi.org/10.1029/93TC03604>
- van Staal, C. R., and de Roo, J. A., 1995, Mid-Paleozoic tectonic evolution of the Appalachian Central Mobile Belt in northern New Brunswick, Canada: Collision, extensional collapse and dextral transpression, in Hibbard, J. P., van Staal, C. R., and Cawood, P. A., editors, *Current Perspectives in the Appalachian-Caledonian Orogen*: Geological Association of Canada, Special Paper 41, p. 367–389.
- van Staal, C. R., and Wilson, R. A., 2014, The Popelogan arc – Tetagouche backarc basin, the Brunswick subduction complex and the Salinic orogeny in northern New Brunswick: *Fredericton, New Brunswick, Canada, Field Trip Guidebook*, Geological Association of Canada/Mineralogical Association of Canada Joint Annual Meeting 2014, 41 p.
- van Staal, C. R., Winchester, J., and Cullen, R., 1988, Evidence for D1-related thrusting and folding in the Bathurst-Millstream River area, New Brunswick, in *Current Research, Part B: Geological Survey of Canada, Paper 88-1B*, p. 135–148.
- van Staal, C. R., Ravenhurst, C. E., Winchester, J. A., Roddick, J. C., and Langton, J. P., 1990, Post-Taconic blueschist suture in the northern Appalachians of northern New Brunswick, Canada: *Geology*, v. 18, n. 11, p. 1073–1077, [http://dx.doi.org/10.1130/0091-7613\(1990\)018<1073:PTBSIT>2.3.CO;2](http://dx.doi.org/10.1130/0091-7613(1990)018<1073:PTBSIT>2.3.CO;2)
- van Staal, C. R., Sullivan, R. W., and Whalen, J. B., 1996, Provenance and tectonic history of the Gander Zone in the Caledonian/Appalachian orogen: Implications for the origin and assembly of Avalon, in Nance, R. D., and Thompson, M. D., editors, *Avalonian and Related Peri-Gondwanan Terranes of the Circum-North Atlantic*: Geological Society of America Special Papers 304, p. 347–367, <http://dx.doi.org/10.1130/0-8137-2304-3.347>
- van Staal, C. R., Dewey, J. F., Mac Niocaill, C., and McKerrow, W. S., 1998, The Cambrian-Silurian tectonic evolution of the northern Appalachians and British Caledonides: History of a complex, west and southwest Pacific-type segment of Iapetus, in Blundell, D. J., and Scott, A. C., editors, *Lyell: The Past is the Key to the Present*: Geological Society, London, Special Publication, v. 143, p. 197–242, <http://dx.doi.org/10.1144/gsl.sp.1998.143.01.17>
- van Staal, C. R., Rogers, N., and Taylor, B. E., 2001, Formation of low temperature mylonites and phyllonites by alkali-metasomatic weakening of felsic volcanic rocks during progressive, subduction-related deformation: *Journal of Structural Geology*, v. 23, n. 6–7, p. 903–921, [http://dx.doi.org/10.1016/S0191-8141\(00\)00163-2](http://dx.doi.org/10.1016/S0191-8141(00)00163-2)
- van Staal, C. R., Wilson, R. A., Rogers, N., Fyffe, L. R., Langton, J. P., McCutcheon, S. R., McNicoll, V., and Ravenhurst, C. E., 2003, Geology and tectonic history of the Bathurst Supergroup, Bathurst Mining Camp, and its relationships to coeval rocks in southwestern New Brunswick and adjacent Maine – A synthesis, in Goodfellow, W. D., McCutcheon, S. R., and Peter, J. M., editors: *Economic Geology Monograph 11*, p. 37–60.
- van Staal, C. R., Whalen, J. B., McNicoll, V. J., Pehrsson, S., Lissenberg, C. J., Zagorevski, A., van Breeman, O., and Jenner, G. A., 2007, The Notre Dame arc and the Taconic Orogeny in Newfoundland: *Geological Society of America, Memoirs*, v. 200, p. 511–552, [http://dx.doi.org/10.1130/2007.1200\(26\)](http://dx.doi.org/10.1130/2007.1200(26))
- van Staal, C. R., Currie, K. L., Rowbotham, G., Rogers, N., and Goodfellow, W., 2008, Pressure-temperature paths and exhumation of Late Ordovician – Early Silurian blueschists and associated metamorphic nappes of the Salinic Brunswick subduction complex, northern Appalachians: *Geological Society of America Bulletin*, v. 120, n. 11–12, p. 1455–1477, <http://dx.doi.org/10.1130/B26324.1>
- van Staal, C. R., Whalen, J. B., Valverde-Vaquero, P., Zagorevski, A., and Rogers, N., 2009, Pre-Carboniferous, episodic accretion-related, orogenesis along the Laurentian margin of the northern Appalachians, in Murphy, J. B., Keppie, J. D., and Hynes, A. J., editors, *Ancient Orogens and Modern Analogues*: Geological Society of London, Special Publications, v. 327, p. 271–316, <http://dx.doi.org/10.1144/sp327.13>
- van Staal, C. R., Barr, S. M., and Murphy, J. B., 2012, Provenance and tectonic evolution of Ganderia: Constraints on the evolution of the Iapetus and Rheic oceans: *Geology*, v. 40, n. 11, p. 987–990, <http://dx.doi.org/10.1130/G33302.1>
- van Staal, C. R., Wilson, R. A., and McClelland, W., 2015, Discussion: Taconian orogenesis, sedimentation and magmatism in the southern Quebec-northern Vermont Appalachians: Stratigraphic and detrital mineral record of Iapetan suturing: *American Journal of Science*, v. 315, n. 5, p. 486–500, <http://dx.doi.org/10.2475/05.2015.04>
- van Staal, C. R., Wilson, R. A., Kamo, S. L., McClelland, W. C., and McNicoll, V., 2016, Evolution of the Early

- to Middle Ordovician Popelogan arc in new Brunswick, Canada and adjacent Maine, USA: Record of arc-trench migration and multiple phases of rifting: *Geological Society of America Bulletin*, v. 128, p. 122–146, <http://dx.doi.org/10.1130/B31253.1>
- Waldron, J. W. F., Floyd, J. D., Simonetti, A., and Heaman, L. M., 2008, Ancient Laurentian detrital zircon in the closing Iapetus Ocean, Southern Uplands terrane, Scotland: *Geology*, v. 36, n. 7, p. 527–530, <http://dx.doi.org/10.1130/G24763A.1>
- Waldron, J. W. F., McNicoll, V. J., and van Staal, C. R., 2012, Laurentia-derived detritus in the Badger Group of central Newfoundland: Deposition during closing of the Iapetus Ocean: *Canadian Journal of Earth Sciences*, v. 49, n. 1, p. 207–221, <http://dx.doi.org/10.1139/e11-030>
- Walker, J. A., 2005, Gilmour Brook South base-metal occurrence, Bathurst Mining Camp, northern New Brunswick, in Martin, G.L., editor, *Geological Investigations in New Brunswick for 2004*: New Brunswick Department of Natural Resources; Minerals, Policy and Planning Division, Mineral Resource Report 2005-01, p. 127–166.
- Whalen, J. B., 1989, The Topsails igneous suite, western Newfoundland: An Early Silurian subduction-related magmatic suite?: *Canadian Journal of Earth Sciences*, v. 26, n. 12, p. 2421–2434, <http://dx.doi.org/10.1139/e89-207>
- Whalen, J. B., McNicoll, V. J., van Staal, C. R., Lissenberg, C. J., Longstaffe, F. J., Jenner, G. A., and van Breeman, O., 2006, Spatial, temporal and geochemical characteristics of Silurian collision-zone magmatism, Newfoundland Appalachians: An example of a rapidly evolving magmatic system related to slab break-off: *Lithos*, v. 89, n. 3–4, p. 377–404, <http://dx.doi.org/10.1016/j.lithos.2005.12.011>
- Williams, H., Lafrance, B., Dean, P. L., Williams, P. F., Pickering, K. T., and van der Pluijm, B. A., 1995, Badger Belt, in Williams, H., editor, *The Appalachian – Caledonian Orogen: Canada and Greenland*: Geological Survey of Canada, *Geology of Canada*, n. 6, p. 403–413 (also *Geological Society of America, Geology of North America*, v. F-1).
- Wilson, R. A., 2003, Geochemistry and petrogenesis of Ordovician arc-related mafic volcanic rocks in the Popelogan inlier, northern New Brunswick: *Canadian Journal of Earth Sciences*, v. 40, n. 9, p. 1171–1189, <http://dx.doi.org/10.1139/e03-034>
- Wilson, R. A., and Kamo, S. L., 2012, The Salinic Orogeny in northern New Brunswick: Geochronological constraints and implications for Silurian stratigraphic nomenclature: *Canadian Journal of Earth Sciences*, v. 49, n.1, p. 222–238, <http://dx.doi.org/10.1139/e11-041>
- Wilson, R. A., Burden, E. T., Bertrand, R., Asselin, E., and McCracken, A. D., 2004, Stratigraphy and tectono-sedimentary evolution of the Late Ordovician to Middle Devonian Gaspé Belt in northern New Brunswick: Evidence from the Restigouche area: *Canadian Journal of Earth Sciences*, v. 41, n. 5, p. 527–551, <http://dx.doi.org/10.1139/e04-011>
- Wilson, R. A., van Staal, C. R., and Kamo, S., 2008, Lower Silurian subduction-related volcanic rocks in the Chaleurs Group, northern New Brunswick, Canada: *Canadian Journal of Earth Sciences*, v. 45, n. 9, p. 981–998, <http://dx.doi.org/10.1139/E08-051>
- Winchester, J. A., van Staal, C. R., and Langton, J. P., 1992, The Ordovician volcanics of the Elmtree-Belledune inlier and their relationship to volcanics of the northern Miramichi Highlands, New Brunswick: *Canadian Journal of Earth Sciences*, v. 29, n. 7, p. 1430–1447, <http://dx.doi.org/10.1139/e92-115>
- Wood, D. A., Joron, J.-L., and Treuil, M., 1979, A re-appraisal of the use of trace elements to classify and discriminate between magma series erupted in different tectonic settings: *Earth and Planetary Science Letters*, v. 45, n. 2, p. 326–336, [http://dx.doi.org/10.1016/0012-821X\(79\)90133-X](http://dx.doi.org/10.1016/0012-821X(79)90133-X)
- Zagorevski, A., van Staal, C. R., McNicoll, V., Rogers, N., and Valverde-Vaquero, P., 2008, Tectonic architecture of an arc-arc collision zone, Newfoundland Appalachians, in Draut, A. E., Clift, P. D., and Scholl, D. W., editors, *Formation and Applications of the Sedimentary Record in Arc Collision Zones*: Geological Society of America, *Special Papers*, v. 346, p. 309–334, [http://dx.doi.org/10.1130/2008.2436\(14\)](http://dx.doi.org/10.1130/2008.2436(14))
- Zagorevski, A., van Staal, C. R., Rogers, N., McNicoll, V. J., and Pollock, J., 2010, Middle Cambrian to Ordovician arc-backarc development on the leading edge of Ganderia, Newfoundland Appalachians: *Geological Society of America, Memoirs*, v. 206, p. 367–396, [http://dx.doi.org/10.1130/2010.1206\(16\)](http://dx.doi.org/10.1130/2010.1206(16))